Master's thesis

NTNU
Norwegian University of Science and Technology
Faculty of Engineering
Department of Manufacturing and Civil Engineering

Yogesh Kaushik

Modeling and RSM Based Multi-Objective Optimization of Product Production Inside CP Factory

Master's thesis in Master's in Sustainable Engineering
Supervisor: Dr. Tamal Ghosh
Co-supervisor: Assoc. Prof. Niels Peter Østbø
July 2022

NTNU
Norwegian University of
Science and Technology

Yogesh Kaushik

Modeling and RSM Based Multi-Objective Optimization of Product Production Inside CP Factory

Master’s thesis in Master's in Sustainable Engineering
Supervisor: Dr. Tamal Ghosh
Co-supervisor: Assoc. Prof. Niels Peter Østbø
July 2022

Norwegian University of Science and Technology
Faculty of Engineering
Department of Manufacturing and Civil Engineering

NTNU
Norwegian University of
Science and Technology

Abstract

CNC milling is a widely used material removal technology in the manufacturing industry. CNC milling can be used for removing extra materials, profiling, slot making, and, in many cases, it could also be used for drilling operations. There were various process parameters that were involved during the milling operation, and these parameters can affect the surface quality of the products as well as their production cost. The objective of this work is to perform parametric optimization based on the different responses. The process parameters like spindle speed, cutting velocity, tool path technology, and overlapping percentage of cutting tool, whereas the responses such as surface roughness, flatness, parallelism, material removal rate (MRR) by weight, and machining time have been taken for this work. The analysis result has been taken from 27 experiments designed using Box-Behnken Design under RSM, and the experiments have been conducted on a micro-CNC milling machine. The results were used in RSM for the analysis and were used by the RSM optimizer to determine the optimal cutting condition based on the responses. The RSM optimizer predicted the optimal parameters condition (spindle speed, cutting velocity, tool path technology, and overlapping percentage of cutting tool) for the best response. Surface roughness 5.07%, flatness 2.5%, parallelism 12.12%, MRR 0.3%, and machining time 0.6% show very close deviations from the predicted value in the validation test.

Sammendrag

CNC maskinering er en materiellfjernings teknologi som er brukt til stor grad i dagens produksjonsindustri. CNC fresing kan bli brukt for å fjerne overskuddsmateriale, frese profiler og spor, og i mange situasjoner drilling. Det var en rekke prosessparametere som var involvert i maskineringen, og disse parameterne kan ha innvirkning på kvaliteten av overflata til produktet, samt den endelige produksjonskostnaden. Målet med dette prosjektet er å utføre parametrisk optimalisering basert på hvordan materialet svarer til ulike freseparametere. Parametere som spindelhastighet, kutthastighet, verktøybaneteknologi og overlapp-prosent av freseverktøyet, hvor responsen fra parametere som overflateujevnheter, flathet, parallellisme, materialfjerningshastighet (MRR) i vekt, samt fresetid har vært fokus i dette prosjektet. Analyseresultatene kommer fra målinger tatt fra 27 forsøk designet ved hjelp av Box-Behnken Design under RSM, og eksperimentene ble gjennomført på en mikro-CNC fres. Resultatene ble brukt i «RSM» til analysen, samt i RSM optimalisering for å fastslå hvilke freseforhold som var mest gunstig basert på de gitte utfallene. RSM optimaliseringen foreslo parametertilstander (spindelhastighet, kutthastighet, verktøybaneteknologi og mengde overlapp på kutthodet) som kunne gi beste mulige sluttresultat. Overflateruhet 5.07%, flathet 2.5%, parallellisme 12.12%, MRR 0.3%, og fresetid 0.6% viser veldig små avvik fra de spådde verdiene i valideringstesten.

Preface

I am highly indebted to my respected supervisors, Dr. Tamal Ghosh and co-supervisor Assoc. professor Niels Peter Østbø for guidance and constant supervision as well as for providing necessary information regarding the project & also for the support in completing the project.

I would like to express my special gratitude and thanks to Mr.Tor Erik Nicolaisen (Laboratory Manager IVB), Mr. Kenneth Kalvåg (Acting Laboratory Manager/Head Engineer) and Pål Erik Endrerud (Staff Engineering) for guiding me on the experiments, machining and testing.

My thanks and appreciations also go to my colleagues in developing the project and people who have willingly helped me out with their abilities to support me throughout my thesis period.

I would like to express my deepest appreciation to all those who provided me the possibility to complete this report. A special gratitude I give to Department of manufacturing and Civil Engineering who helped me to coordinate my project by providing me a good environment. I will always be debated to Norwegian University of Science and Technology for providing this opportunity to learn and polish my skill. A special thanks goes to my parents and sister for their continuous support and encouragement.

At last, but not least, I would like to thank SFI manufacturing for supporting this project and the Project No. is 237900 and is funded by the Research Council of Norway (RCN).

Yogesh Kaushik

2022

Table of Contents

List of Figure

List of Table

List of Abbreviations

CNC	Computer Numeric Control	GRA	Grey Relational Analysis
MRR	Material Removal Rate	RSM	Response Surface Method
Ra	Surface Roughness	GA	Genetic Algorithm
CE	Cutting Energy	PSO	Particle Swarm Optimization
SS	Spindle Speed	BPNN	Back Propagation Neural Network
FR	Feed Rate	ACO	Ant Colony Optimization
DOC	Depth of Cut	ANFIS	Adaptive Neuro-Fuzzy Inference
WOC	Width of Cut		System
Rz	Maximum profile height	FEM	Finite Element Method
CF	Cutting Force	SVM	Support Vector Machine
SCF	Specific Cutting Force	NSGA	Non-dominated Sorting Genetic
FPT	Feed Per Tooth	II	Algorithm II
CS	Cutting Speed	CS	Cuckoo Search
NP	Number of Passes	RBF	Radial Basis Function
ADOC	Axial Depth of Cut	PCA	Principal Component Analysis
RDOC	Radial Depth of Cut	TOPSIS	Technique for Order of Preference
RRA	Radial Rake Angle		by Similarity to Ideal Solution
HA	Helix Angle	UT	Utilization Theory
TW	Tool Wear	FFNN	Feed Forward Neural Network
TNR	Tool Nose Radius	MRPI	Multi Response Performance Index
ARET	Axial Run-out Errors of each	TS	Tabu Search
RRET	Tooth	GSO	Glowworm Swarm Optimization
CV	Radial Run-out Errors of each	GOA	Grid Optimization Algorithm
IA	Tooth	DF	Desirability Function
S_q	Cutting Vibration	ANN	Artificial Neural Network
σ_x, σ_y	Inclination Angle	RPD-	Robust Parameter Design-RSM
PVD	3D Surface Roughness	RSM	Augmented-enhanced normalized
CVD	Residual Stress along x and y	AENNC	normal constraint
MSIA	Physical Vapor Deposition	GWO	Gray Wolf Optimizer
NR	Chemical Vapor Deposition	WLS	Weighted Least Squares
ACE	Machined Surface Inclination	NNC	Normalized Normal Constraint
MC	Angle		
MT	Nose Radius		
DA	Air Cutting Energy		
SEC	Machining Cost		
TL	Machining Time		
TOL	Dimensional Accuracy		
FLR	Specific Energy Consumption		

FW SF SH TS NC SL IE TC MTH	Tool Life Tool Overhang Length Flow Rate Flank Wear Static Force Surface Hardness Toolpath Strategy Nanoparticle concentration Spindle Load Insert Edge Total Cylindricity Metamorphic Thickness		

1. Introduction

One of the most popular machining processes, milling involves intricate interactions between the workpiece and the cutting tools as well as patterns of chip generation. In order to avoid defects in the end product such as surface flaws, profile errors, damage to the cutting tools, and even damage to the milling machine itself, it is crucial to choose the milling process settings carefully [1].

Due to increased pressure from global competition, manufacturers must develop ways to boot bot h efficiency and product quality [2], Efficiency in the use of machining has always been an issue, and when CNC milling machines are employed, this issue becomes more complicated due to the high number of process parameters and high initial investment costs [3]. Currently, a lot of work is being done to increase productivity and machining by taking into account social factors like worker safety as well as product quality and energy usage. One of the most widely employed methods among all the efforts was parametric optimization, which involved conducting a task using the optimal machining settings to produce a better-quality result.

Since milling is a material removal process, the product's surface quality always plays a significant part in the milling operation since certain features may determine both the output of the machined product and its production cost. Similarly, flatness and parallelism play a significant part when higher precision is required in the finished product, MRR and machining time play a significant role in milling operations because they affect the overall machining run time, which is directly related to production costs.

There are various parameters used in milling operation but out of all these the parameters such as cutting velocity, spindle speed, tool path technology and tool overlapping percentage act as a major influencer on the surface quality of the products as well as its productivity and the production time.

In the past, the machining parameters were chosen by trial and error, which is time-consuming, not very cost-efficient, and always requires highly competent and experienced operators. The chosen parameters were also only effective for a limited number of operations. This demonstrates the significance of optimizing the machining process parameters for improved product accuracy and increased productivity.

To solve the problem of optimization several methods were proposed, the methods like factorial design, Taguchi method, response surface methodology etc, were the most common methods that were used. With the help of these methods, design of experiment was prepared by including the different process parameters with their levels to conduct the experiment and further the prediction and optimization of that process were carried out with respect to the response characteristic.

RSM is one of the most commonly used methods for the optimization of multiple response, it is a synergy of statistical, mathematical and analytical which identify the synchronous effects of several design variables on the overall system performance [4].

The present study includes studies of end milling process parameters to get better surface quality with higher MRR by weight and less machining time to make the CNC end milling process more sustainable. The responses, surface roughness, flatness, and parallelism are treated as quality indicators, whereas the MRR and machining time are treated as indicators for productivity and production cost. The product that has been machined is the mobile back cover. The product is used in the CP factory for the process demonstration.

1.1. Thesis structure

There are 6 chapters in this thesis.

The first chapter is an introduction to the research, with a motivation for using various process parameters and different response parameters to conduct multi-objective optimization of CNC milling in order to make the milling process more sustainable.

The second chapter is for literature review, to get the state-of-the-art in the study area and to find possible research gaps.

The third chapter presents the experimental procedure, which includes material, machining process, process and response parameters, test methods, and analysis and optimization tools.

The fourth chapter is a result and discussion, which presents the result in the form of a response and their analysis and optimization with validation.

The fifth chapter is where the conclusion of the overall thesis has been made.

The sixth chapter is for future scope, where the few new ideas related to this work have been pointed out.

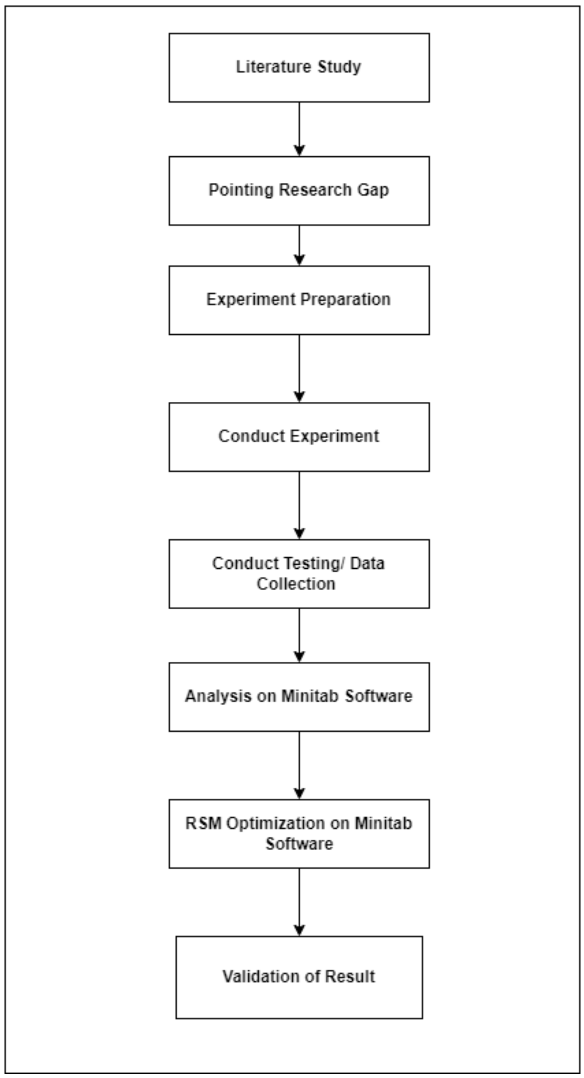

Figure 1.1:1: Structure of thesis

2. Literature study

To get the proper insight and current development of the selected study area a small literature search and review has been carried out by following some general literature review guidelines. The time frame for the literature study has been kept between 2010 to January 2022. After shortlisting the relevant studies, all the data were kept in data matrix so that the result from the literature could be clearer to understand. The search of the articles has been caried out on Google scholar database. The given below steps are the general steps that were taken in account to get relevant source for the study:

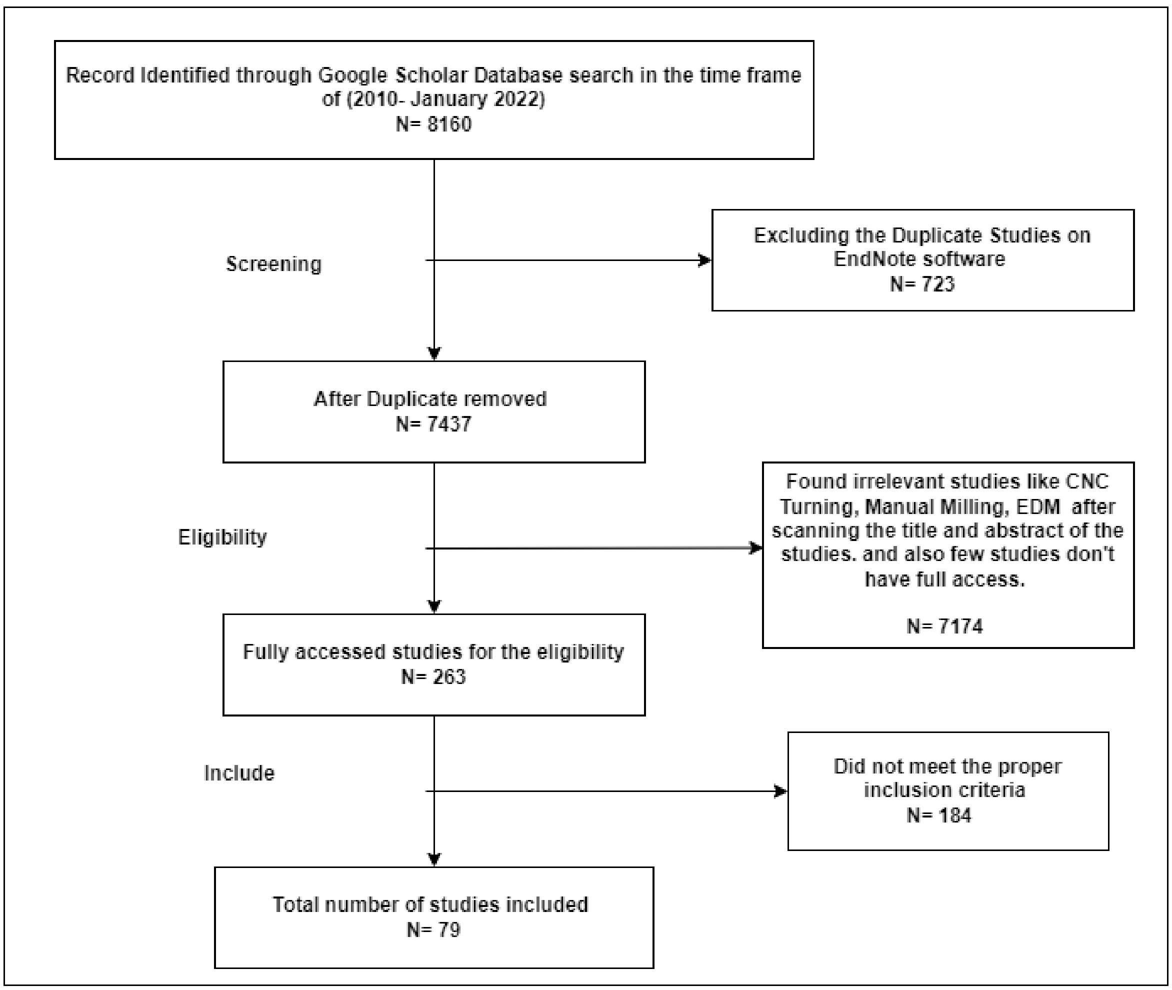

Figure 1.1:1: Summary of data collection

2.1. Identification

This is the first stage, where the literature was searched on the Google Scholar database. While searching, keywords such as "multi-objective optimization," "prediction model," "CNC," "CNC Milling Machine," "Surface Roughness," have been used. The search gave a total of 8160 hits.

2.2. Screening and Eligibility

At this stage, first the duplicate papers were removed with the help of EndNote software, and then a rapid study of the titles and abstracts of the articles was carried out. After this, a total of 263 articles were selected for further processing.

2.3. Final includes

At this stage, all the selected articles from the previous stage were studied thoroughly, focusing more on the experimental part, the analysis part, and the model used for prediction and optimization. After this, a total of 79 articles were included in the literature review study.

2.4. Data matrix

Ref.	Machine Make and Model	Tool Type	Cutting Materials	No. of Responses	Process Parameters	Process Responses	Prediction Model	Optimization Model
[5]	6-axes Haans machining centre	End Mill	AA6061-T6	1	CS, FR, ADOC, RDOC	Ra	RSM	ACO
[6]	Deckel Maho DMU 70 V	End Mill	polyamide-6	2	NC Content, FR, SS	Ra, CF	BPNN	PSO
[7]	Hurco CNC BMC-20LR	Face Mill	Medium Carbon Steel C45	3	SS, FR, DOC, and WOC	MRR, Ra, CE	–	Taguchi-GRA
[8]	DECKEL MAHO DMU 60 P CNC	Ball End Mill	Al 7075	3	SS, FR, DOC	TW, CF, Ra	Regression	GRA
[9]	vertical CNC	Face Mill, End Mill	10 L50 leaded steel	3	CS, FR	CE, Ra, CF	Mathematical Model	CS
[10]	Hass-US 5-axis CNC	End Mill	Inconel 718	2	CS, FR, DOC	Ra, MRR	–	GRA
[11]	Johnford VMC 850	Face Mill	AISI 1050 steel	3	DOC, CS, FR, Coolant	Temperature, Ra, CF	BPNN	Taguchi Method
[12]	Makino S33	End Mill	Al 7075 T6	2	CS, FR, DOC, NR	Ra, MRR	–	Fuzzy MRPI
[13]	ProLight2000	End Mill	Brass (60/40)	1	CS, FR, DOC	Ra	ANFIS	–
[14]	Vertical CNC	Ball End Mill	Al2014-T6	3	FPT, ADOC, RDOC, CS	Three CF components	RSM	GA
[15]	MCV 350	Face Mill	Hadfield steel GX120Mn14	2	CS, FR, Tools	Ra, TW	Regression	Taguchi Method
[16]	OKUMA CNC	End Mill	Al-epoxy hybrid composite	2	SS, FR, DOC	Ra, CF	–	Taguchi Method
[17]	LV65	End Mill	Aluminium	2	DOC, FR, SS	Ra, MRR	–	PCA, PCA-UT, PCA-GRA, PCA-TOPSIS
[18]	–	End Mill	Al6061	1	SS, FR, DOC	Ra	FFNN	–
[19]	AJAX AJ540	End Mill	D2 steel	3	CS, DOC, FR	Ra, energy	Regression	GA
[20]	SPINNER U-620	End Mill	S50C steel	2	MSIA, ADOC, SS, FR	microhardness and residual stress	–	Taguchi Method
[21]	Johnford VMC550	Face Mill	AA7039, Al_2O_3	2	CS, FPT, DOC	Ra, CF	FFNN	Taguchi Method
[22]	VMC0540d	Face Mill	Al 7050	1	ARET, RRET, CF, CV, FR	Ra	Mathematical Model	–
[23]	VM-10 of HURCO	End Mill	EN-31 steel	3	CS, FPT, DOC	Ra, TW, Vibration	Regression	RSM
[24]	Deckel Maho, DMV 50 evolution	End Mill	Al 7075-T7351	1	CS, FR, ADOC, TNR	Ra	Geometrical Model	–
[25]	MTAB	End Mill	Metal Matrix Composite	2	CS, FR, DOC	Ra, Fc	Regression	Fuzzy GRA
[26]	Johnford VMC 550 model CNC	End Mill	AISI 1050 steel	3	CS, FR, DOC, # of inserts	Vibration, CF, Ra	Regression	GRA
[27]	BFW, Model UF-1	End Mill	AA6082T6	2	SS, FR, DOC	MRR, Roughness	ANFIS	Fuzzy-GRA
[28]	–	End Mill	Ti6Al4V	1	CS, FPT, DOC, WOC	CF	FEM, SVM, BPNN	NSGA II
[29]	PL700	End Mill	AISI 1045 steel	1	SS, FPT, DOC, WOC	SEC	RSM	MOPSO
[30]	DMU 65 monoBlock	End Mill	AISI type 304 steel	1	DOC, FR, SS	CE	RSM	RSM

[31]	FANUC MCV 400	End Mill	Aluminum bar	1	CS, FR, DOC	Ra	Regression	GSO
[32]	heavy-duty double column	End Mill	cast iron HT250	4	SS, DOC, FR	MC, MT, DA, CE	Mathematical Model	GOA
[33]	Mitsui Seiki, VT3A	End Mill	S50C steel	3	SS, FR, DOC, MM, CFL	Residual Stress, CF, Ra	RSM	RSM
[34]	Bridgeport VMC 610	End Mill	Ti-6Al-4V	5	CS, FR, DOC, Environment	Ra, TL, CE, SEC	–	Taguchi Method
[35]	Generic	End Mill	P20 steel	2	NR, CS, FR, ADOC, RDOC	MRR, Ra	RSM	Taguchi Method, RSM
[36]	Spark DTC 250	End Mill	AA6061	3	SS, FR, DOC	CF, RA, CE	RSM	PSO
[37]	FVP-800	Ball End Mill	Inconel 718	3	CS, FR, IA	S_q, σx, σy	RBF	GRA, PSO
[38]	ZXX6350ZA	End Mill	St52 and Al 7075	3	SS, FR, ADOC	Ra, Vibration	Perceptron	–
[39]	BHARAT FRITZ WERNER BF-1	End Mill	Al7075	4	SS, FR, DOC, % of SiC	CF, Ra, MRR, TW	RSM	GRA
[40]	ALMO	Face Mill	stainless steel X2CrNi18-9	5	CS, FPT, DOC	Ra, CF, SCF, MRR, CE	RSM	DF
[41]	VGC1500	Face Mill	S45C steel	2	CS, FR, DOC, WOC	SEC, PC	Mathematical Model	AMOPSO
[42]	Deckel Maho DMC 63V	End Mill	steel GMTC 1.2738	1	CS, FR, RDOC	Ra	–	Taguchi Method
[43]	SMART MILL 500	End Mill	Ti–6Al–4V	7	CS, FR, DOC	MRR, CE, Ra, CF, TW, Current	RSM	RSM, GA
[44]	Johnford VMC550	Face Mill	Al7075, SiC foam-reinforced Al7075	1	CS, FR, ADOC	Ra	ANN, Regression	–
[45]	FADAL VMC 15	End Mill	AISI 1045 steel	2	CS, FR, ADOC, RDOC	Ra, MRR	RSM	Weighted PCA
[46]	DECKEL MAHO DMU 60	End Mill	Ti6Al4V, Inconel 718	4	SS, FR, DOC	Ra, TW, CF	Regression	Taguchi Method
[47]	X6132A	End Mill	AISI 1060	3	CS, FR, Air Condition	Ra, CF, SEC	RSM	RSM
[48]	Romi Discovery 560	End Mill	Al 7075	3	CS, axial FPT, TOL	TR, MRR, CF	RPD-RSM	AENNC, TOPSIS
[49]	KVC800	End Mill	C45 Steel	3	CS, FR, COD, WOC	TL, Ra, CE	Mathematical Model	GA
[50]	JYOTI vertical CNC	End Mill	Al 7068	1	CS, FR, ADOC, HA, RRA	Temperature	Polynomial Regression	GA
[51]	MDX 540	End Mill	green alumina	1	CS, SS, DOC	Ra	Regression	GA
[52]	HASS TM2	Ball End Mill	Inconel 718	3	CS, FR, DOC, NP	CF 3 components	Regression	GA
[53]	Johnford VMC550	End Mill	AA7039 B_4C and SiC	1	CS, FR, DOC	Ra	ANN, RSM, Regression	Taguchi Method
[54]	5 Axis CNC	Ball End Mill	55NiCrMoV6 steel	2	CS, FR, DOC, SS	CF, Vibration	Regression	Taguchi-GRA
[55]	–	Micro End Mill	AISI 304 stainless steel	3	SS, FPT, DOC	Ra, FW, Cutter Vibration	–	Taguchi Method, GTMA, Utility Concept
[56]	DECKLE CNC	Ball End Mill	6061-T6	2	Vibration Amplitude, FR, SF	Ra, SH	Regression	FEM, RSM, Desirability Function
[57]	MTAB	End Mill	Al2024-T4	3	SS, FR, DOC	MRR, Ra, CF	BPNN	Taguchi Method

[58]	Deckel Maho DMU 50	Ball End Mill	Ti-6Al-4V	1	CS, RDOC, FPT	Ra	Regression	Taguchi Method
[59]	Sunlike 7.5 bhp CNC	End Mill	AISI 4140 steel	2	FR, CS, FLR	SEC, Ra	RSM	Taguchi Method
[60]	Kuka QUANTECKR120R2700	End Mill	Al6005A	2	TS, FR, SS	SR, MT	–	Taguchi-GRA
[61]	HAAS VF-3YT	Ball End Mill	steel X210CR12	1	SS, FR, ADOC, RDOC	Ra	RSM	GA, GWO
[62]	CNC vertical Center	End Mill	Ti-6Al-4V	3	SS, DOC, FPT	Ra, BH-DM, BH-UM	Regression	GRA
[63]	HAAS VF-2 CNC	End Mill	6061 T6	3	ADOC, FPT, CS	SEC, Ra	RSM	RSM, Desirability Test
[64]	SmartOne 500	End Mill	AISI 1045 steel	3	SS, DOC, WOC, FR	MRR, CE, ACE	Nonlinear Regression	TS
[65]	Carver 400M_RT	Face Mill	AISI 1045 steel	3	SS, FR, DOC, WOC	MRR, Ra, ACE	RSM	Taguchi-GRA, NSGA II
[66]	Haas VF-2 CNC	End Mill	AISI 1018 steel	3	CS, DOC, FR, NC	SL, IE, Ra	Regression	Taguchi Method
[67]	C-TEK CNC KM80D	Face Mill	AL2024-T4	2	CS, FR, DOC, TS	Ra, MRR	RSM	RSM, GRA
[68]	ROMI® Discovery 560	End Mill	AISI H13	3	CS, axial FPT, tangential FPT	TR, TC, Ra	Regression WLS	NNC, WLS
[69]	KERN Evo ultra-precision	End Mill	alumina composite	3	SS, ADOC, FPT	Ra, CF, TW	–	Taguchi-GRA, TOPSIS
[70]	QJK006	Disc Mill	TC4 alloy	3	SS, FR, DOC	MRR, TL, MTH	RSM	RSM, GRA
[71]	ARIX VMC 100	End Mill	6082-T6	5	CS, FR, Air Condition	Ra, CF, Temperature	–	Taguchi-TOPSIS
[72]	3 Axis CNC SIEMENS802D BMV 40 320D controller	End Mill	Aluminium Metal Matrix Composite	6	SiC Size, CS, FR, DOC	MRR, Ra, CF, Temperature	Regression, ANN	GRA
[73]	EPO07R012M	End Mill	SKD61	3	DOC,SS,FR,Nose radius	Ra, Cutting energy, Roughness depth	Kriging Model	AMGA
[74]	3 Axis CNC Dry mill	End Mill	AA6061,AA2024,AA7075	2	FPT, CS	CF,Ra	ANFIS	PSO,GA
[75]	Sandvik R245-063Q22	Face Mill	Grade-H steel	1	SS,FR,DOC	Ra	ANN	Edgeworth, Pareto Frontiers
[76]	3 Axis CNC Siemens 810D	End Mill	Inconel 738	2	CS,FR,Coolent , ADOC	CF,Ra	ANN	GA
[77]	BFW SURYA VF30 CNC VS	End Mill	AISI H11	2	CS,FR,DOC	Ra, MRR	Regression	Taguchi-GRA
[78]	Proxxon FF 500/BL 3 Axis CNC	End Mill	AA3105	3	TD,FR,SS,DOC	MMR,Ra,CF	KSOM	GRA, VIKOR,BRNN-BAS, Regression-BAS
[79]	JDLVG600_A10	End Mill	SS7050	2	CS, FPT, ADOC, RDOC	CF,Ra	RSM	RSM, TLBO
[80]	CNC VMC (YCM 1020)	End Mill	AL6060-SiC-Gr	1	FR,DOC,CS	Ra	Linear Regression	Taguchi method
[81]	DAEWOO ACE-V500	Face Mill	CGI	2	DOC,FPT,CS	CF,Ra	NANFIS	IPOS, NANFIS
[82]	SIEG 3/10/0016	End Mill	AL8112	3	SS,DOC,FR,Length of Cut	Ra,MRR,CF	Mathematical Model, QRCCD	ORCCD
[83]	VMC580E CNC	End Mill	Al Alloy	3	SS,CS,DOC,CW	Ra,SEC,MT	Regression	GA

2.5. Synthesis

2.5.1. Year wise study

The line chat below presents the record of the number of studies published in the respective year. It can also show the trend of this study area showing significant growth between 2016 to 2019. In 2017, there were the highest number of studies done on the multi-objective parameter optimization of CNC milling with 15 studies done out of 79, whereas there was no most relevant study performed in 2012.

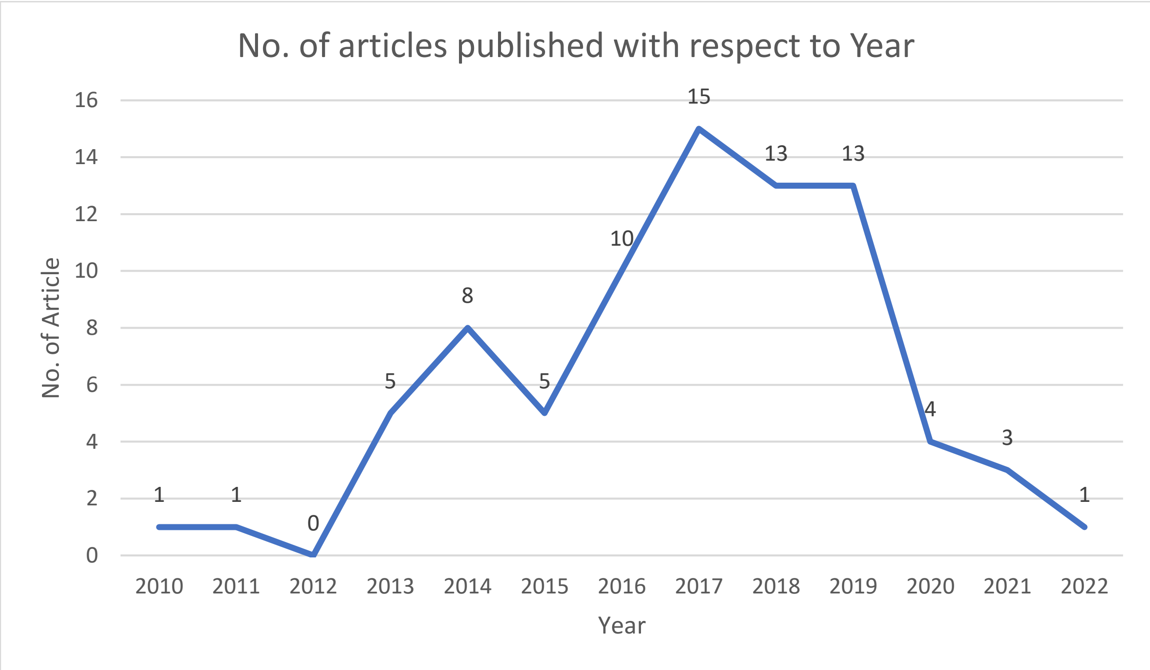

Figure 2.5:1 year wise publication

2.5.2. Milling type

The type of milling used is also an important consideration in milling operations. There were various types of milling done according to the requirements, but out of all these, end milling and face milling are the most widely used milling techniques. And the synthesis of data from the data matrix proves the same. In 60 out of 78 studies, the experiment was performed using the end milling technique followed by face milling. In some studies, the authors used two different techniques in their experiments. whereas disk milling has been used in just one study out of 79 studies.

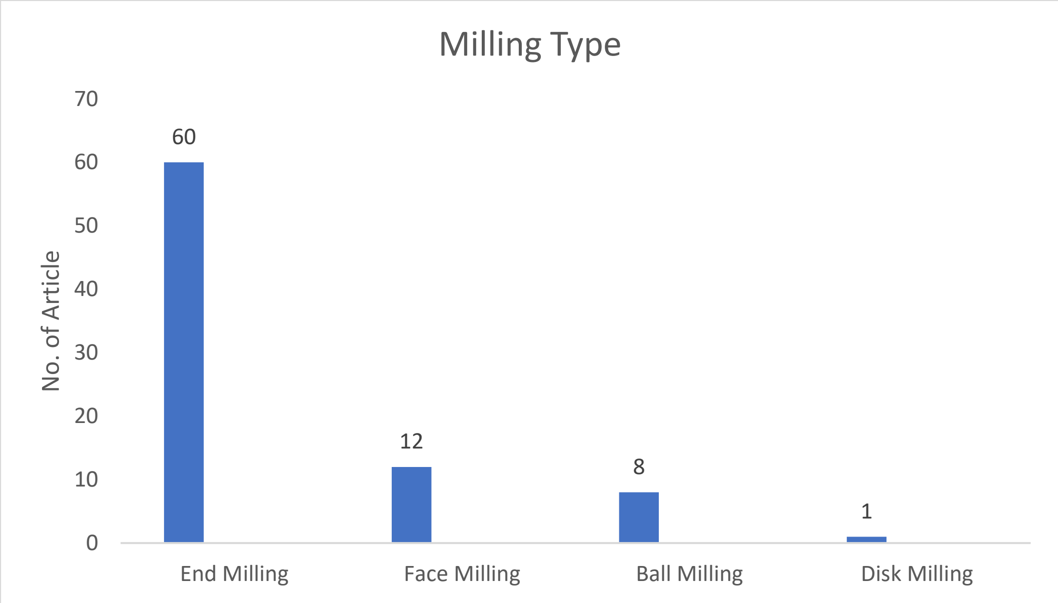

Figure 2.5:2 Milling Type

2.5.3. Workpiece material

When it comes to the workpiece material, the majority of the studies were conducted on aluminum alloy and steel. 29 studies had used aluminum alloy, while 26 studies had used steel. Out of 79 studies, brass was used in one study. Brass has good machinability properties and is widely used in the manufacturing domain. The very limited use of brass as a workpiece for the CNC milling process has given one motivation to carry out the experiment for this study on brass.

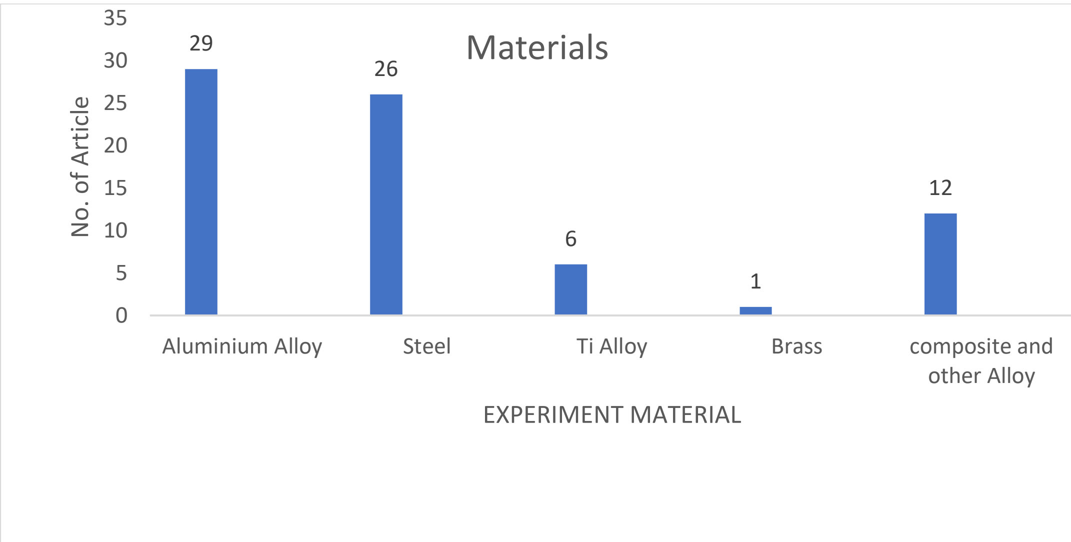

Figure 2.5:3 Material used in different literature

2.5.4. Process parameter

Process parameters are the parameters that can be controlled and manipulated while performing the experiment. The majority of the studies have used three or four process parameters in their experiments. 43 out of 79 studies used three process parameters. The most common parameters that were found in almost all studies are feed rate, depth of cut, and spindle speed. This demonstrates that these parameters have a significant impact on the response parameters. very least, studies have used parameters such as tool path technology and overlapping percentage of cutting tool (cutting width). From the data matrix, it can be found that only one study out of 79 studies has included cutting width in their process parameters, while two out of 79 studies have used tool path technology as their process parameters. The small number of studies conducted while using these two process parameters indicates a type of research gap, and this gap has been solved in this study.

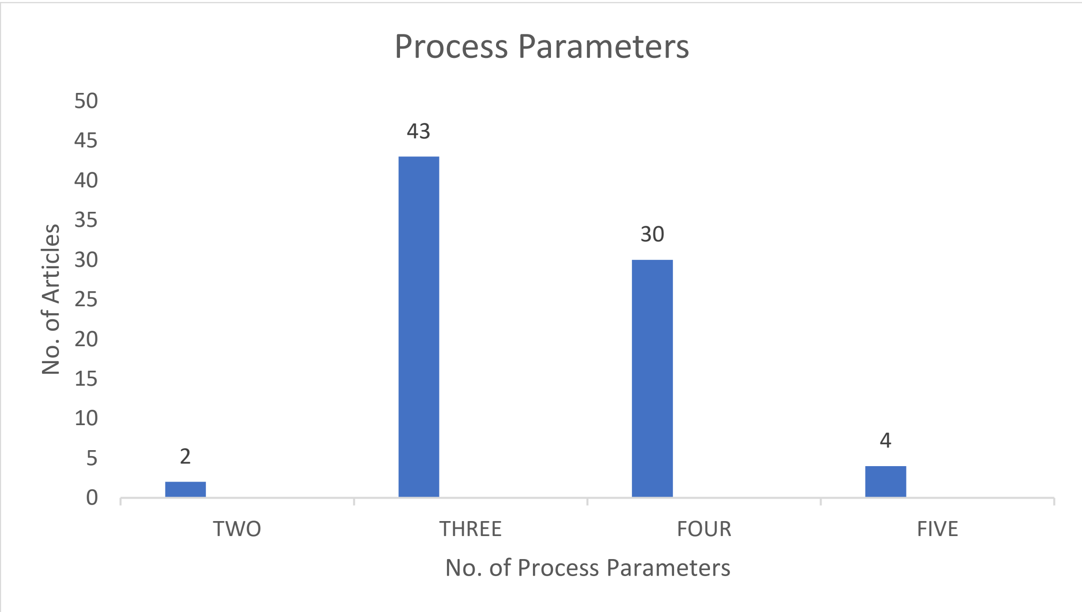

Figure 2.5:4 No. of process parameters

2.5.5. Response parameters

The majority of the studies were conducted using 1 to 3 response parameters. 30 out of 79 studies used 3 different response parameters. And one of the widely used response parameters was surface roughness. Various other parameters like MRR and cutting force have also been used in most studies. But there is a lack of various other surface characteristic features in almost every study. Almost 80.013% of the studies have used surface roughness to illustrate the surface quality, but still there were various other surface features that could be taken into account when referring to the surface quality, features like the flatness of the surface, the perpendicularity of the surface, as well as the parallelism of the machined surface. To solve this gap, in this study, five different response parameters have been used: surface roughness, MRR by weight, machining time, flatness, and parallelism.

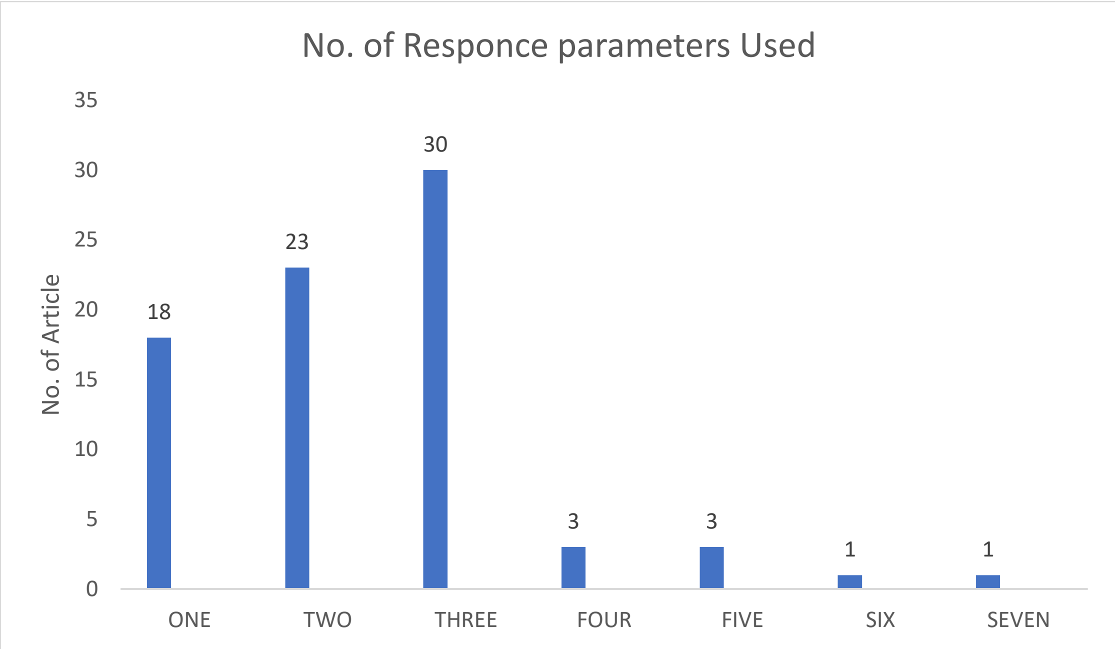

Figure 2.5:5 No. of Response parameters

3. Experiment Procedure

3.1. Material

The workpiece material used for the experiments is brass alloy. The brass alloy with 2% of lead which gives a good chips removal as well as its allies with good machinability [84]. The chemical, mechanical, and physical properties of the material are shown below:

Chemical Properties (%) [84]:

Material	Cu	Pb	Fe	Ni	Sn	Al	Zn	Other
Value	58-60	1.6-2.5	0-0.3	0-0.3	0-0.3	0-0.05	remaining	0-0.2

Table 3.1-1 Chemical Properties of Brass alloy

Mechanical Properties *[84]*:

Tensile strength (Mpa)	Yield strength (Mpa)	Elastic modulus (Gpa)	Elongation in two inches
360	140	108	45

Table 3.1-2 Mechanical Properties of Brass alloy

Physical Properties [84]:

Thermal Expansion Coefficient [10-6/K]	Electrical Conductivity [% IACS]	Thermal Conductivity [W/ (m.K)]	Density [g/cm3]
20.9	24	110	8.46

Table 3.1-3 Physical Properties of Brass alloy

The dimension of the brass alloy plate used in the experiments is 160mm length* 80mm width* 15mm thickness.

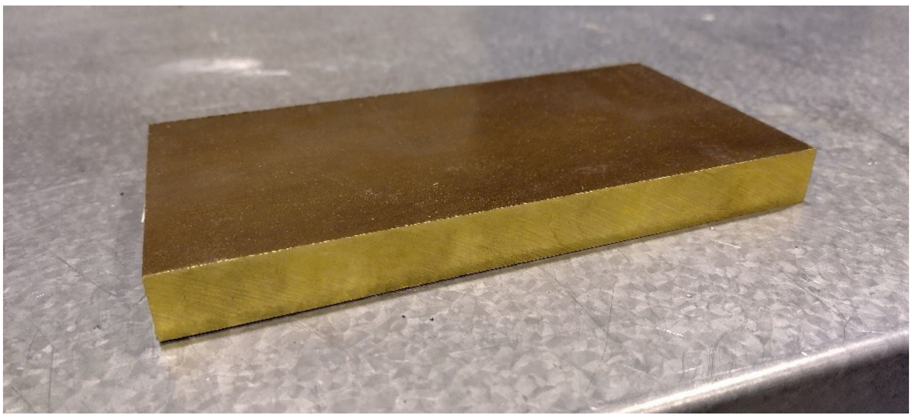

Figure 3.1:1 Workpiece

3.2. Process Parameters

Total 4 different parameters have been chosen to perform the machining. The parameters were selected after finding some research gap from the literature studies. The parameters are spindle speed, cutting velocity, overlapping percentage and tool path technology.

3.2.1. Spindle Speed

spindle speed is one of the important parameters used while milling operation. Either the milling operation is conventional manual mill or CNC mill, spindle speed plays high impact on the machining performance. It is the speed at which the spindle rotates. The cutting tool is attached to the spindle, so typically spindle speed is the speed at which the tool rotates during milling operation. The formula used to find the spindle speed is shown in equation below:

$$N = \frac{V * 1000}{\pi * D}$$

Where, N is the spindle speed in rpm, V is the cutting velocity in meter/minute and D is the diameter of the cutting tool in mm.

3.2.2. Cutting Velocity

The rate at which the cutting tools moves the material is known as cutting velocity. It is the movement of cutting tool in X-direction and Y-direction on the workpiece.

3.2.3. Overlapping Percentage

It is a machining parameter in which the milling tool overlap with the mentioned percentage on the initial machined area. For example, if the diameter of the tool is 12mm and the overlapping percentage is 50%, then when the tool starts machining, going from X-positive direction to X-negative direction, at first the tool removes the material according to its real diameter which is 12mm, but again while returning the tool act like 6mm, the tool only removes 6mm width of material. Figure 3.2:1, illustrate the tool path generated with different overlapping percentage. Higher the overlapping percentage will be, less the no. of tool path will be for that respective design.

3.2.4. Tool Path Technology

It is a set of coordinates positions which the milling tool can follow throughout the machining operation [85]. There were various types of different tool path technologies used for specific machining, but the most common tool path technology used is counter tool path technology. The various other tool path technology are zigzag, helical, spiral etc. In the figure-3.2:1 , were the example of different tool path technology that has been used in the experiment.

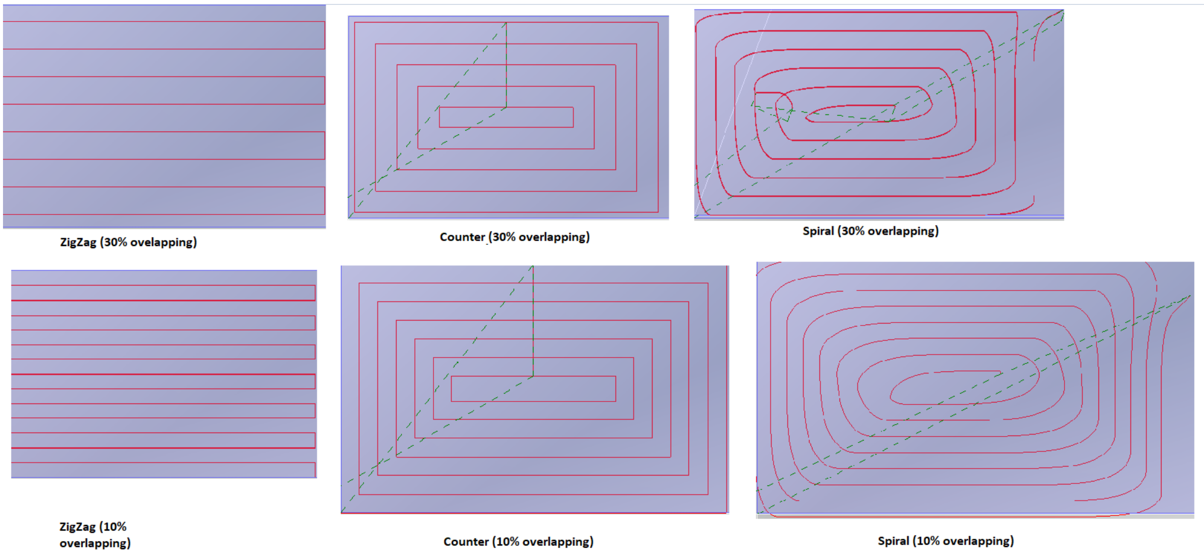

Figure 3.2:1 Tool Path with Overlapping Percentage

3.3. Specimen 3d design

3.3.1. 3D design

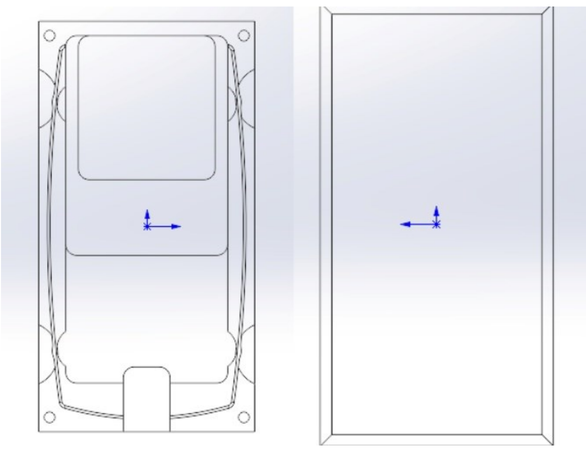

Figure 3.3:1 SolidWorks 3D Design of Specimen

The 3D model used in this study has been provided by the Festo. The product is a mobile cover which is used in cyber physical factory for the process demonstration.

3.3.2. SolidCam

This software is used as a post processor. The reason behind using SolidCam is because it gives flexibility to modify the parameters, such as overlapping percentage and tool path technology. The G-code is also generated on the SolidCam software. But the G-code generated from SolidCam needed to be modified so that it can run on NCCAD 9. The G-code for each experiment is presented in appendix-A.

3.4. Response Surface Methodology (RSM)

Box and Wilson created the Response Surface Methodology (RSM), which is a group of mathematical and statistical tools whose goal is to evaluate situations using an empirical model and aims to relate a response to the amount of various input variables or factors that influence it through suitable experiment design and analysis [86] [87]. The flow chart of step used in RSM(Box-Behnken design) is presented in the figure 3.4:2

3.4.1. Box-Behnken Design

The experiment for this study was performed using Box-Behnken Design as a response surface method. The Box-Behnken design (BBD) model is more appropriate for many scientific applications among the several types of RSM models that have so far been developed because of its improved accuracy, resilience, dependability, and need for less computing. The BBD model also has the advantage of maintaining all design points inside the parameters set by the designer for the chosen design elements. The most general version of the regression equation that was created during the development of the BBD model to correlate the inputs and outputs involves individual inputs, an interaction between the inputs, and the square of inputs to increase the precision of the projected outcomes [88]. These layouts don't rely on full or partial factorial layouts. The design points are located in the center of the dimension k-1 subareas. For instance, in the case of three factors, the points are situated at the center of the experimental domain's edges [89]. Figure 3.4:1 is the example of 3 factor Box-Behnken Design [90].

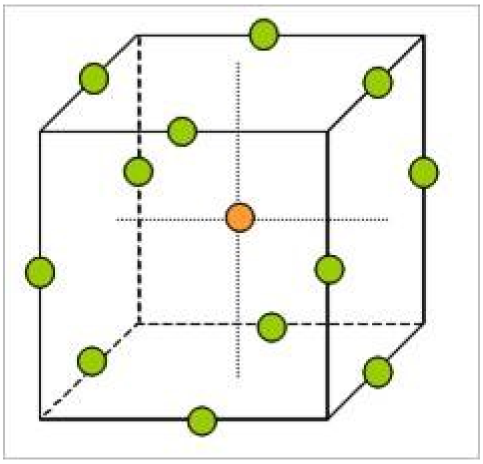

Figure 3.4:1 Graphical Representation of 3-factor Box-Behnken Design

The Box-Behnken design required three level for each factor. The three level of each factor for this current work has been shown in the table 3.4-1. If the nature of relationship between the response parameter(Y) and the process parameters(X) is known the model is written in the simple equation [91]:

$$Y = (X_1 + X_2 + X_3 + X_4 \dots + X_n) + \epsilon$$

Where, ϵ is the error related with the response(Y).

Similarly, if we present the response like the below equation [91]:

$$E(Y) = (X_1 + X_2 + X_3 + X_4 \dots + X_n) + \eta$$

Then the representation of the surface will be [91]:

$$\eta = (X1 + X2 + X3 + X4 \dots . Xn)$$

And η , here is the surface response. But in general, the surface response uses the second-order model which is presented below in the form of equation [91] [92]:

$$Y = \beta_0 + \sum_{i=1}^{k} \beta_i X_i + \sum_{i=1}^{k} \beta_{ii} X_i^2 + \sum_{i} \sum_{j} \beta_{ij} X_i X_j + \varepsilon$$

Where, Y is the predicted response, β_0 is the constant coefficient, β_i is the linear coefficient, β_{ii} is the quadratic coefficient, β_{ij} is the interaction coefficient whereas, X_i and X_j is the factors. The Box-Behnken design for the four factors with three level is given in the table below.

Run	Block	A	B	C	D
1	1	-1	-1	0	0
2	1	1	-1	0	0
3	1	-1	1	0	0
4	1	1	1	0	0
5	1	0	0	-1	-1
6	1	0	0	1	-1
7	1	0	0	-1	1
8	1	0	0	1	1
9	1	-1	0	0	-1
10	1	1	0	0	-1
11	1	-1	0	0	1
12	1	1	0	0	1
13	1	0	-1	-1	0
14	1	0	1	-1	0
15	1	0	-1	1	0
16	1	0	1	1	0
17	1	-1	0	-1	0
18	1	1	0	-1	0
19	1	-1	0	1	0
20	1	1	0	1	0
21	1	0	-1	0	-1
22	1	0	1	0	-1
23	1	0	-1	0	1
24	1	0	1	0	1
25	1	0	0	0	0
26	1	0	0	0	0
27	1	0	0	0	0

Table 3.4-1 Box-Behnken Design

Parameter	Lower Range (-1)	Middle Range (0)	Upper Range (1)
Overlapping percentage (%)	10	30	50
Spindle speed(rpm)	1800	2150	2500
Cutting velocity (m/min)	70	80	90
Toolpath	Counter	Zig-zag	Spiral

Table 3.4-2 Parameters with their Range (Level)

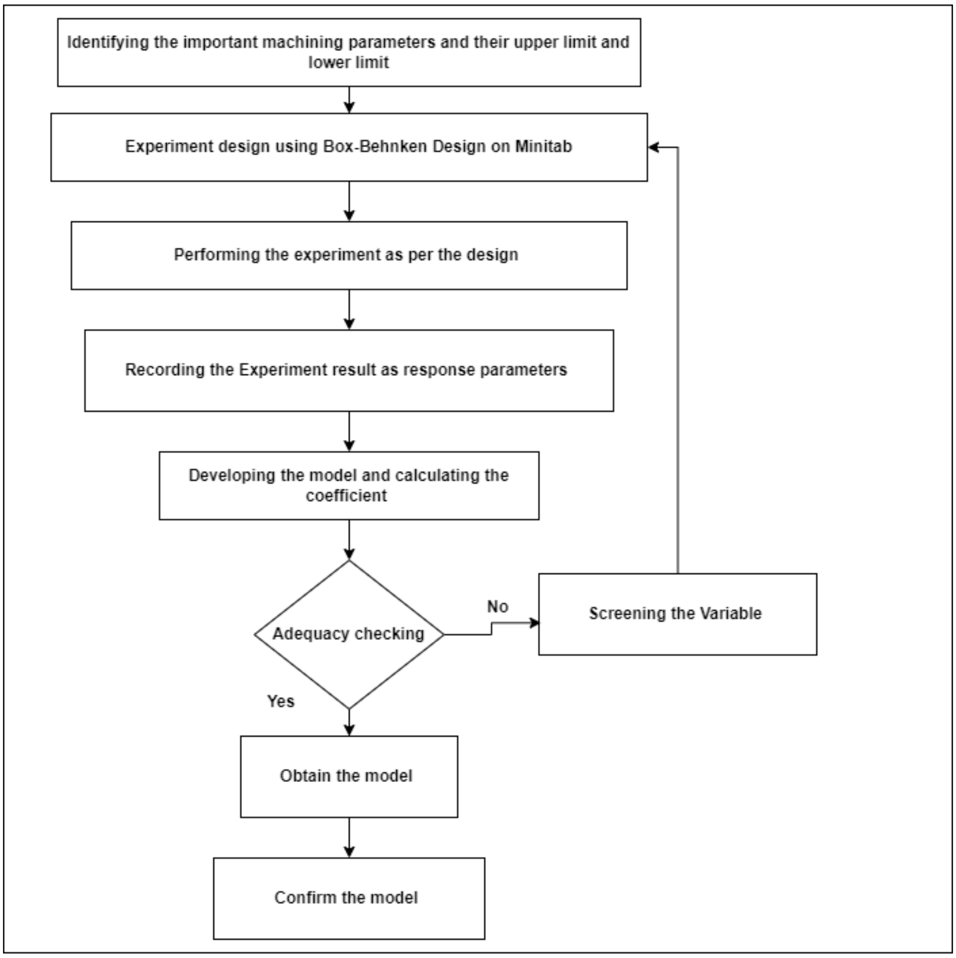

Figure 3.4:2 Flow chart of working of Box-Behnken Design

3.4.2. Design of Experiment

Total 27 experiment were performed. With the Minitab software and following Response Surface methodology (RSM) strategy all the 27 experiments with above mentioned parameters were generated. The process parameters are arranged like A= Overlapping percentage, B= Spindle speed, C= Cutting velocity and D= Tool path. The experiments list is presented below:

Run No.	Overlapping percentage	Spindle Speed	Cutting Velocity	Tool Path Technology
1	10	1800	80	ZIG-ZAG
2	50	1800	80	ZIG-ZAG
3	10	2500	80	ZIG-ZAG
4	50	2500	80	ZIG-ZAG
5	30	2150	70	COUNTER
6	30	2150	90	COUNTER
7	30	2150	70	SPIRAL
8	30	2150	90	SPIRAL
9	10	2150	80	COUNTER
10	50	2150	80	COUNTER
11	10	2150	80	SPIRAL
12	50	2150	80	SPIRAL
13	30	1800	70	ZIG-ZAG
14	30	2500	70	ZIG-ZAG
15	30	1800	90	ZIG-ZAG
16	30	2500	90	ZIG-ZAG
17	10	2150	70	ZIG-ZAG
18	50	2150	70	ZIG-ZAG
19	10	2150	90	ZIG-ZAG
20	50	2150	90	ZIG-ZAG
21	30	1800	80	COUNTER
22	30	2500	80	COUNTER
23	30	1800	80	SPIRAL
24	30	2500	80	SPIRAL
25	30	2150	80	ZIG-ZAG
26	30	2150	80	ZIG-ZAG
27	30	2150	80	ZIG-ZAG

Table 3.4-3 Experiment Design

3.5. Machining

CNC milling is one of the most common materials removing process used nowadays. This experiment is performed on a micro milling machine. The general specification of the CNC milling machine used in this project is given below:

Parameters	Value
Machine Tag Name	Proxxon FF500 CNC
Country of origin	Germany
Number of axis	3-axis (X, Y and Z)
Working table dimension	290mm*100mm
Peak Spindle speed	4000 RPM
Software used for controller	NCCAD 9 Mill

Table 3.5-1 Specification of micro-CNC milling machine

End milling tool with 12mm tool diameter has been used to machine the flat surface (the surface that being studied) while 4 mm tool is used to make the extra profile in all 27 experiments. The machining is carried out to make a mobile back cover. The machining setup is shown in the figure 3.5:1.

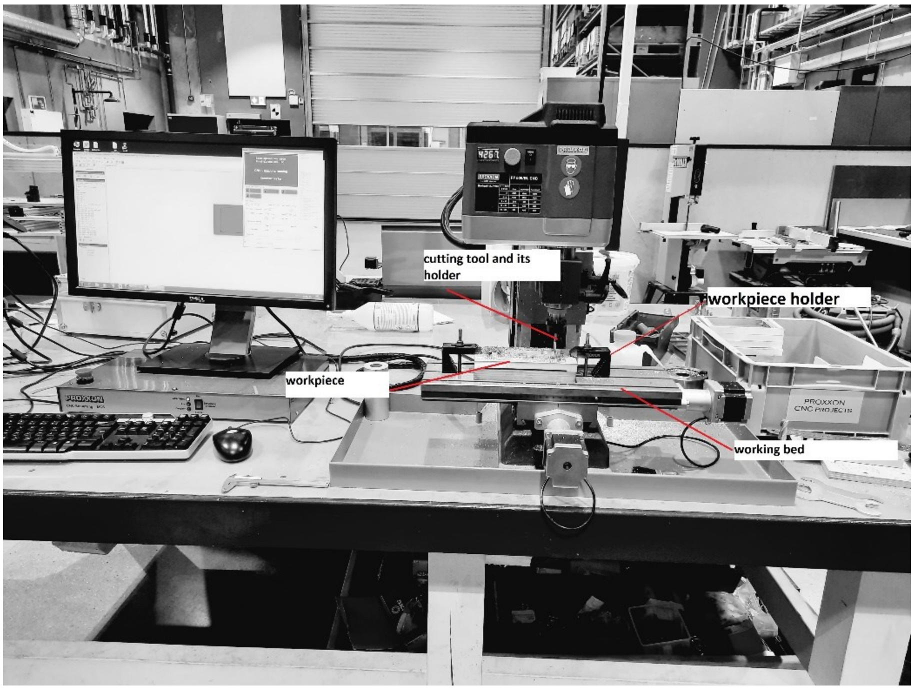

Figure 3.5:1 Machining Setup

The milling bed is of T-slots type and the clamp used for holding the workpiece is step clamps. The clamp used to hold the tool in the milling machine head is a precision spring collect clamp for 12mm diameter tool. Milling of brass alloy generally required very less amount of lubricant/coolant and all the experiment were performed without any lubricant/coolant. The depth of cut has been kept constant to 0.6mm throughout all the experiments.

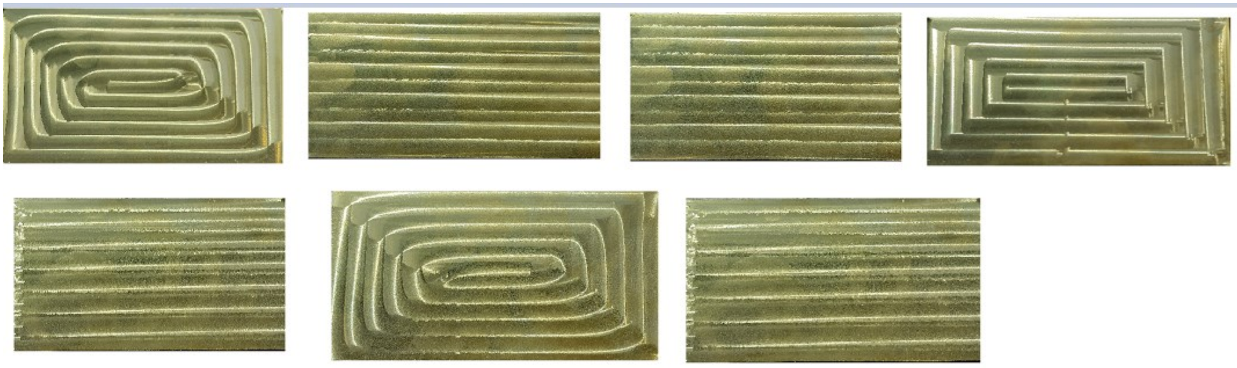

Figure 3.5:2 Machined Specimen

The above image is the surface of mobile back cover which has been studied in this work.

3.6. Response and their Testing

3.6.1. Material Removal Rate (MRR)

To calculate the Material Removal Rate (MRR) by weight. The Initial Weight of the material and the weight of the material after milling has been noted. The material removal rate by weight is thus calculated using given formula:

MMR= (Initial weight of workpiece- weight of material after milling)/ Total time taken for milling

Experiment No.	Initial Weight (gm)	Final Weight (gm)
1	1665	1368
2	1648	1366
3	1668	1384
4	1645	1362
5	1642	1368
6	1646	1372
7	1644	1362
8	1640	1356
9	1644	1378
10	1646	1360
11	1638	1360
12	1642	1344
13	1648	1368
14	1656	1376
15	1650	1366
16	1656	1370
17	1654	1372
18	1646	1358
19	1646	1360
20	1642	1358
21	1646	1370
22	1660	1380
23	1642	1362
24	1644	1364
25	1650	1365
26	1654	1370
27	1650	1362

Table 3.6-1 weight of material before and after experiment

3.6.2. Surface Roughness

The arithmetic mean deviation of a profile (Ra) was the most commonly used parameter, and it was accepted by the majority of standards organizations. Ra is the arithmetic mean of the absolute value of the distance between the profile and the baseline within the specific length [92]. A contract profilometer was used to measure the surface roughness. The profilometer is from a company called Zeiss with the tag name of Handysurf E-35B. Figure 3.6:2 portray the measurement setup of surface roughness using handysurf.

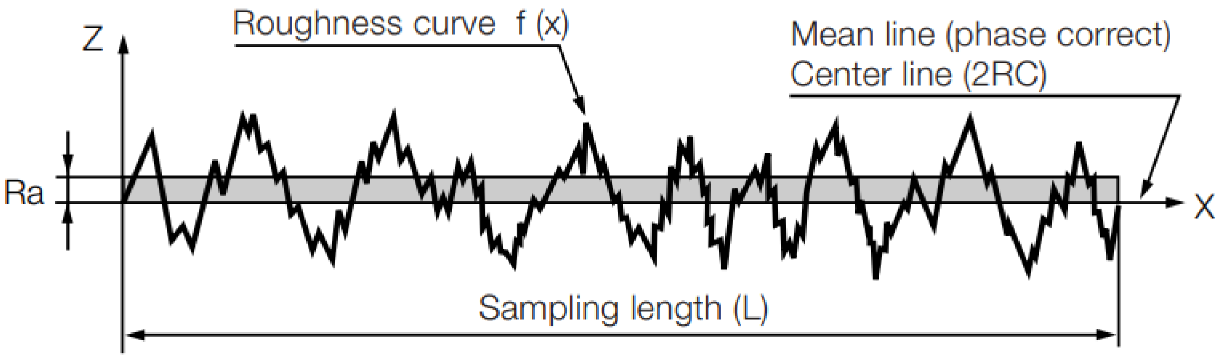

Figure 3.6:1 arithmetic average deviation representation *[93]*

The handysurf is a contract-based measurement system where the stylus used to travel on the measuring profile surface. The stylus tip is made up of diamond and the radius if the tip is 5µm with the measuring resolution of 0.0007µm [94]. This profilometer only measure the surface roughness of very small area, but the sample size used for the experiment is large, so to get the overall surface roughness of the sample, five randomly points was selected and at every point, consecutive 3 measurement were carried out and then the overall all mean of all the recorded value of surface roughness was kept as the final surface roughness value of the sample

Figure 3.6:2 Handysurf doing surface measurement

3.6.3. Flatness

Flatness lies under form geometric tolerance, which is the uniformity of the surface, or the medium plane as required. Flatness cannot be measured by simply placing some gauge or instrument over the surface. To find the flatness we must have to compare it with a reference feature parallel to the sample that is to be measure.

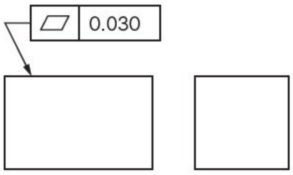

Figure 3.6:3 Reference symbol for flatness *[95]*.

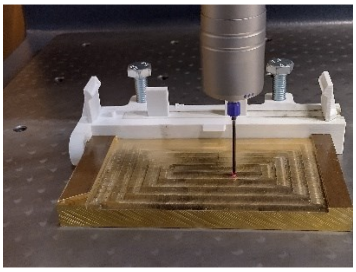

Figure 3.6:4 CMM and its prob

To measure the flatness, Coordinate Measuring Machine (CMM). A virtual reference feature was created with the help of 3D design of the sample and then with the help of CMM the sample surface was compared with the 3D design. This gave the variation recorded by the prob of the CMM and this variation came in the form of tolerance.

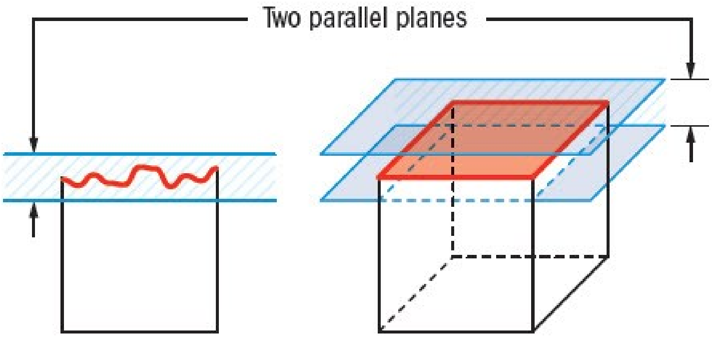

Figure 3.6:5 Two parallel planes for comparison *[95]***.**

The Coordinate Measuring Machine used in this experiment is from a company named Zeiss, and the model's name of the machine is DuraMax. The CMM had been fully calibrated before the measurement. The calibration was conducted by the Zeiss company's representative on May 17th, 2022, and the measurements were performed on May 24th, 2020. The radius of the probe used in this experiment is 1.5mm. A measurement plan for the flatness was programmed on the Zeiss Calypso software with a total of 1932 measurement points and an automatically generated plot. Figure 3.6:6 is the representation of the plot, and the measurements result from the flatness of Experiment-1. The plots diagram of rest all experiment has been kept in AppendixB.

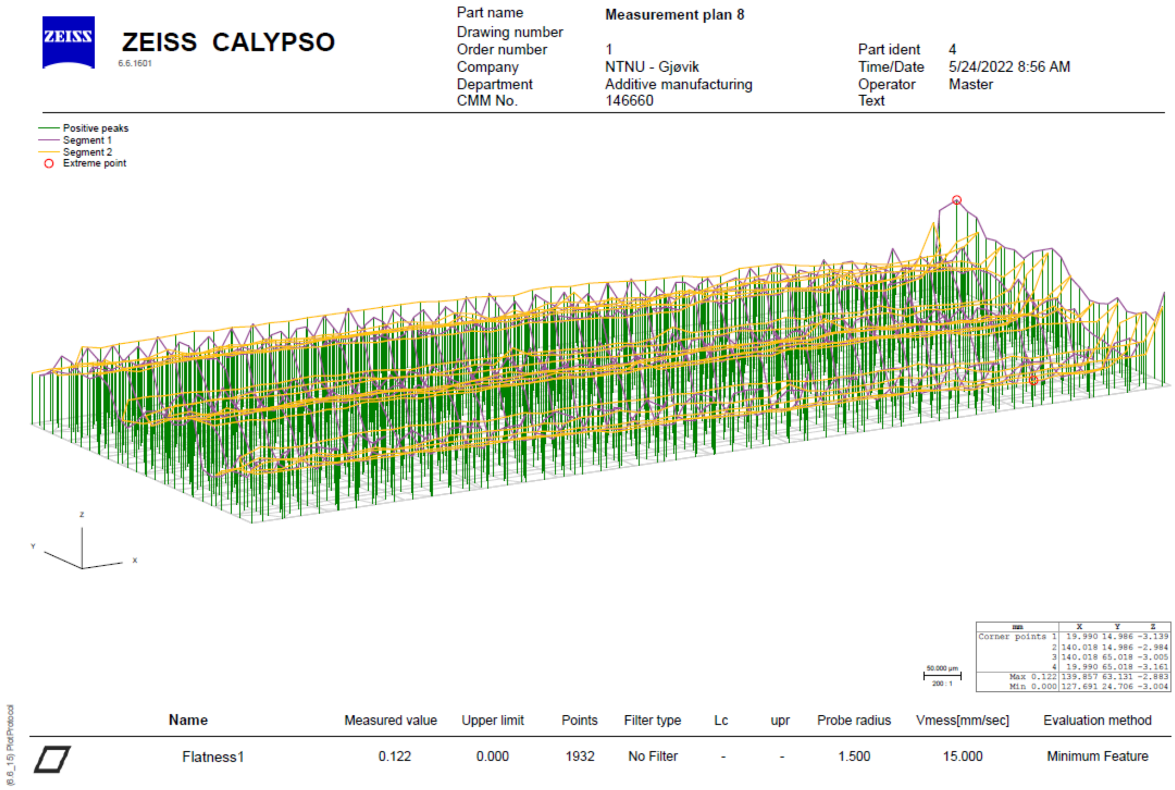

Figure 3.6:6 Plot diagram for flatness of experiment 1

3.6.4. Parallelism

parallelism is one of the terms used in geometrical dimensioning and tolerancing which controls the requirement for two planes or features to be geometric parallel with each other's, within some acceptable tolerance. It always required some geometry or reference features to compare the parallelism with each other's.

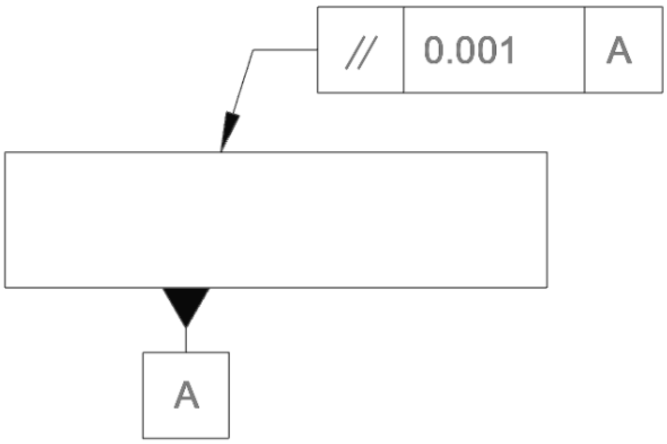

Figure 3.6:7 Reference symbol of parallelism *[96]*

The measurement of parallelism has been carried out by following the same procedures that were used while measuring the flatness on the CMM. To parallelism in these experiments were measured by comparing the casted plane and the plane obtained after the machining.

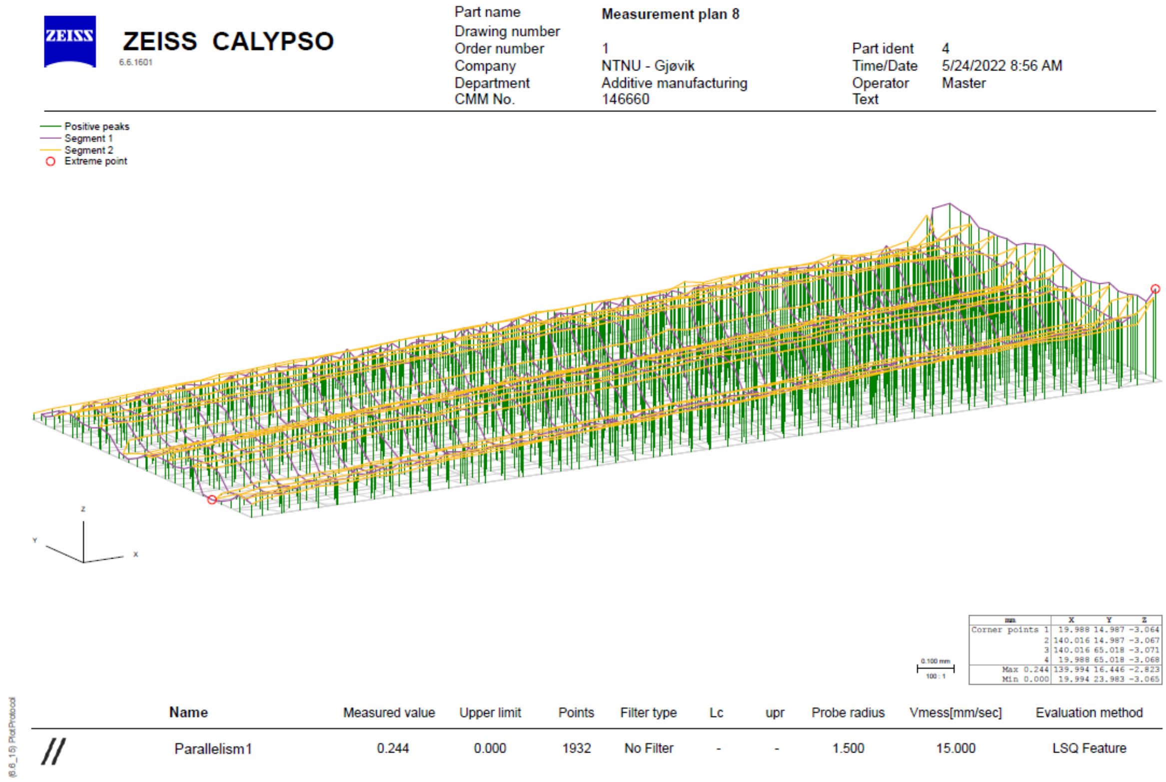

Figure 3.6:8 Plot diagram for parallelism for experiment 1

3.6.5. Machining Time

Machining time is the total run time of the CNC milling machine while machining the workpiece. The time was measure in two different ways. The first way is by using mobile stopwatch and the second way is to see the machine run time on the controller software.

4. Result and Discussion

4.1. Material Removal Rate (MRR)

Run No.	Overlapping percentage	Spindle Speed	Cutting Velocity	Tool Path Technology	MRR
1	10	1800	80	ZIG-ZAG	0.2072
2	50	1800	80	ZIG-ZAG	0.1222
3	10	2500	80	ZIG-ZAG	0.2039
4	50	2500	80	ZIG-ZAG	0.1224
5	30	2150	70	COUNTER	0.1363
6	30	2150	90	COUNTER	0.1667
7	30	2150	70	SPIRAL	0.1715
8	30	2150	90	SPIRAL	0.1646
9	10	2150	80	COUNTER	0.1612
10	50	2150	80	COUNTER	0.1133
11	10	2150	80	SPIRAL	0.1764
12	50	2150	80	SPIRAL	0.1137
13	30	1800	70	ZIG-ZAG	0.1471
14	30	2500	70	ZIG-ZAG	0.1473
15	30	1800	90	ZIG-ZAG	0.1865
16	30	2500	90	ZIG-ZAG	0.1876
17	10	2150	70	ZIG-ZAG	0.1802
18	50	2150	70	ZIG-ZAG	0.1114
19	10	2150	90	ZIG-ZAG	0.2281
20	50	2150	90	ZIG-ZAG	0.1382
21	30	1800	80	COUNTER	0.1538
22	30	2500	80	COUNTER	0.1562
23	30	1800	80	SPIRAL	0.1439
24	30	2500	80	SPIRAL	0.144

25	30	2150	80	ZIG-ZAG	0.1644
26	30	2150	80	ZIG-ZAG	0.1636
27	30	2150	80	ZIG-ZAG	0.1661

Table 4.1-1 Material Removal Rate (gm/sec) for the 27 experiments

4.2. Surface Roughness and Machining Time

Exp. No.	Overlapping percentage	Spindle speed	Cutting Velocity	Tool Path Technology	Surface Roughness (Ra)	Machining Time (Sec.)
1	10	1800	80	ZIG-ZAG	1.864	1385
2	50	1800	80	ZIG-ZAG	1.62	2308
3	10	2500	80	ZIG-ZAG	1.43	1393
4	50	2500	80	ZIG-ZAG	0.996	2312
5	30	2150	70	COUNTER	1.576	2010
6	30	2150	90	COUNTER	1.316	1644
7	30	2150	70	SPIRAL	1.564	2284
8	30	2150	90	SPIRAL	1.632	1725
9	10	2150	80	COUNTER	1.552	1650
10	50	2150	80	COUNTER	1.436	2525
11	10	2150	80	SPIRAL	1.47	1576
12	50	2150	80	SPIRAL	1.96	2620
13	30	1800	70	ZIG-ZAG	1.008	1904
14	30	2500	70	ZIG-ZAG	0.938	1900
15	30	1800	90	ZIG-ZAG	1.44	1523
16	30	2500	90	ZIG-ZAG	2.402	1524
17	10	2150	70	ZIG-ZAG	1.848	1665
18	50	2150	70	ZIG-ZAG	1.494	2586
19	10	2150	90	ZIG-ZAG	2.106	1254
20	50	2150	90	ZIG-ZAG	1.9	2055
21	30	1800	80	COUNTER	1.608	1795
22	30	2500	80	COUNTER	1.376	1793
23	30	1800	80	SPIRAL	2.21	1945
24	30	2500	80	SPIRAL	1.6	1944
25	30	2150	80	ZIG-ZAG	2.008	1734
26	30	2150	80	ZIG-ZAG	2.015	1736
27	30	2150	80	ZIG-ZAG	1.992	1734

Table 4.2-1 Surface Roughness and Total Machining Time for 27 experiments

4.3. Flatness and Parallelism

Exp. No.	Overlapping percentage	Spindle speed	Cutting Velocity	Tool Path Technology	Flatness	Parallelism
1	10	1800	80	ZIG-ZAG	0.122	0.244
2	50	1800	80	ZIG-ZAG	0.072	0.096
3	10	2500	80	ZIG-ZAG	0.104	0.11
4	50	2500	80	ZIG-ZAG	0.053	0.054
5	30	2150	70	COUNTER	0.095	0.118
6	30	2150	90	COUNTER	0.106	0.205
7	30	2150	70	SPIRAL	0.097	0.156
8	30	2150	90	SPIRAL	0.1	0.171
9	10	2150	80	COUNTER	0.134	0.145
10	50	2150	80	COUNTER	0.066	0.114
11	10	2150	80	SPIRAL	0.124	0.217
12	50	2150	80	SPIRAL	0.084	0.236
13	30	1800	70	ZIG-ZAG	0.05	0.06
14	30	2500	70	ZIG-ZAG	0.77	150
15	30	1800	90	ZIG-ZAG	0.061	0.098
16	30	2500	90	ZIG-ZAG	0.058	0.2
17	10	2150	70	ZIG-ZAG	0.082	0.225
18	50	2150	70	ZIG-ZAG	0.052	0.206
19	10	2150	90	ZIG-ZAG	0.083	0.219
20	50	2150	90	ZIG-ZAG	0.057	0.095
21	30	1800	80	COUNTER	0.096	0.131
22	30	2500	80	COUNTER	0.098	0.203
23	30	1800	80	SPIRAL	0.097	0.217
24	30	2500	80	SPIRAL	0.102	0.231
25	30	2150	80	ZIG-ZAG	0.058	0.237
26	30	2150	80	ZIG-ZAG	0.059	0.238
27	30	2150	80	ZIG-ZAG	0.058	0.24

Table 4.3-1 Flatness and Parallelism for 27 experiments

4.4. Surface roughness Vs Overlapping percentage, Spindle speed, cutting velocity and tool path

The model summary:

S	R-sq	R-sq(adj)	R-sq(pred)
0.373567	51.66%	0.00%	0.00%

Table 4.4-1 Model summary for surface roughness

The value of R-sq is 51.66% which shows the response surface roughness fits 51.66% in the model. 55.66% of the variability can be observed by the surface roughness.

The ANOVA analysis for surface roughness against process parameters are given below:

Analysis of Variance

Source	DF	Adj SS	Adj MS	F-Value	P-Value
Model	14	1.78949	0.127821	0.92	0.567
Linear	4	0.82010	0.205024	1.47	0.272
overlapping percentage	1	0.06221	0.062208	0.45	0.517
spindle speed	1	0.08467	0.084672	0.61	0.451
cutting velocity	1	0.46729	0.467285	3.35	0.092
tool path	1	0.20593	0.205932	1.48	0.248
Square	4	0.53421	0.133553	0.96	0.465
overlapping percentage*overlapping percentage	1	0.10566	0.105656	0.76	0.401
spindle speed*spindle speed	1	0.44468	0.444675	3.19	0.100
cutting velocity*cutting velocity	1	0.20751	0.207507	1.49	0.246
tool path*tool path	1	0.18800	0.188000	1.35	0.268
2-Way Interaction	6	0.43518	0.072531	0.52	0.783
overlapping percentage*spindle speed	1	0.00902	0.009025	0.06	0.804
overlapping percentage*cutting velocity	1	0.00548	0.005476	0.04	0.846
overlapping percentage*tool path	1	0.09181	0.091809	0.66	0.433
spindle speed*cutting velocity	1	0.26626	0.266256	1.91	0.192
spindle speed*tool path	1	0.03572	0.035721	0.26	0.622
cutting velocity*tool path	1	0.02690	0.026896	0.19	0.668
Error	12	1.67463	0.139553		
Lack-of-Fit	10	1.67435	0.167435	1204.57	0.001
Pure Error	2	0.00028	0.000139		
Total	26	3.46412			

Table 4.4-2 ANOVA between Surface Roughness and process parameters

According to the model, the Lake-of-fit of overall model after conducting ANOVA analysis is 0.001, which is less than 0.05. This suggests that the model is not statically significant at 95% of the confidence interval. The overall model is 43.3% true out of 95%, but when going through the individual parameters' interaction with the surface roughness, the overlapping percentage is 48.3% true instead of being 95% true, the spindle speed is 54.9% true instead of being 95% true, the cutting velocity is 90.8% true instead of being 95% true, and the tool path is 75.2% true instead of being 95% true. This means that the parameters, cutting velocity and tool path, have higher interaction on the response surface roughness compared to the other two process parameters, i.e., overlapping percentage and spindle speed. But going through the square factor, the ANOVA results show that the square factor of spindle speed (spindle speed* spindle speed) has a p-value of 0.100 which is 90% true instead of 95% true, which means that the square factor of spindle speed has a lot of variance over surface roughness when compared to other process parameter's square factors.

Similarly, the two-way interaction suggests that the interaction between overlapping percentage and cutting velocity has more impact on the surface roughness, with the P-value of 0.04 making this interaction statistically significant, followed by the two-way interaction between overlapping percentage and spindle speed with a P-value of 0.06 (94% true instead of 95%).

The empirical relation between surface roughness (Ra,µm) and process parameters is expressed as follows:

*Roughness = -10.1 + 0.0173 overlapping percentage + 0.00420 spindle speed + 0.171 cutting velocity - 0.17 tool path - 0.000352 overlapping percentage*overlapping percentage - 0.000002 spindle speed*spindle speed - 0.00197 cutting velocity*cutting velocity - 0.188 tool path*tool path - 0.000007 overlapping percentage*spindle speed + 0.000185 overlapping percentage*cutting velocity + 0.00758 overlapping percentage*tool path + 0.000074 spindle speed*cutting velocity - 0.000270 spindle speed*tool path + 0.0082 cutting velocity*tool path*

.

The residual plots shown in the figure4.4:1, state that the residuals follow approximately a straight line with high number of residuals very close to the line, indicates the normal distribution of the residual. The residual vs observation plot shows no obvious pattern therefor there is no violation of the uncorrelated variance in the model.

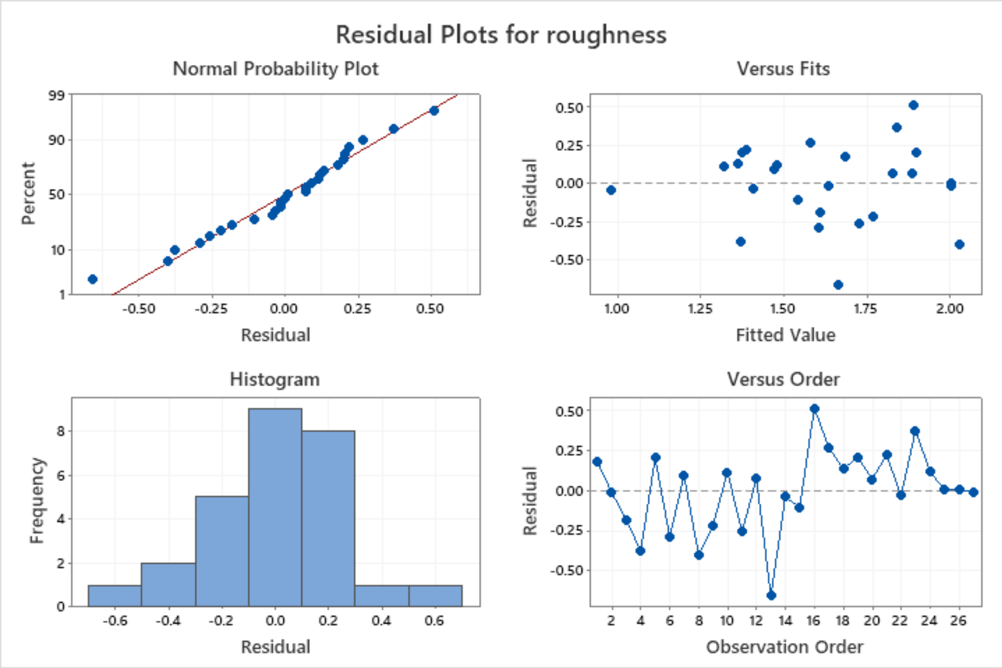

Figure 4.4:1 Residual Plots for surface roughness

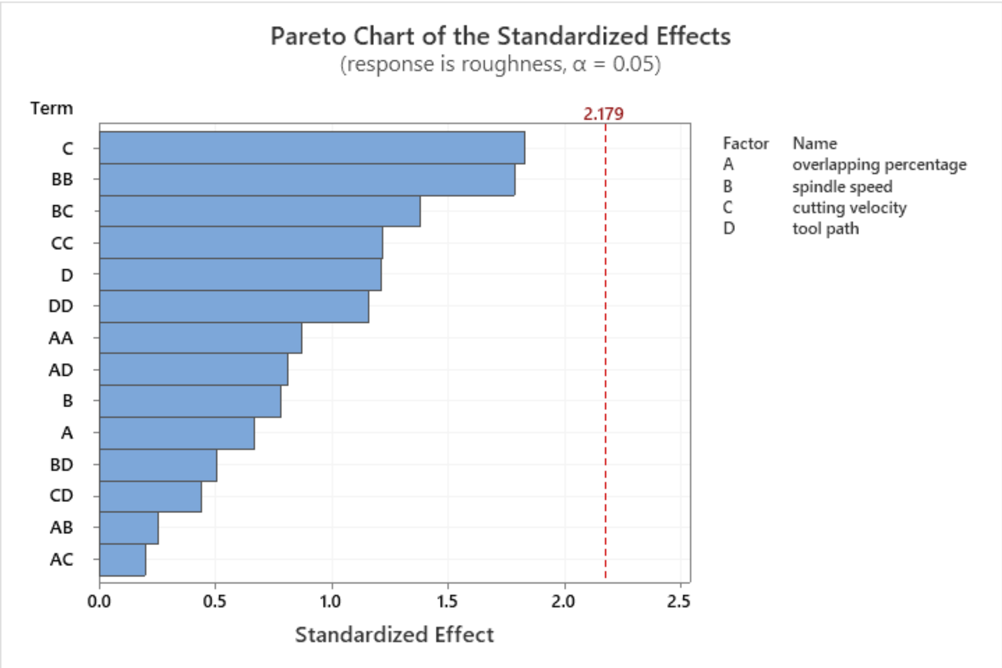

Figure 4.4:2 Pareto Chart for surface roughness

According to the pareto chart for the response surface roughness, at alpha= 0.05, there is no any effect that are influencing the surface roughness much because of the process parameters, but according to the chart, the factor cutting velocity, the square factor of spindle speed and square factor of spindle speed and cutting velocity have the tendency to cause effect on the surface roughness.

4.5. Flatness Vs Overlapping percentage, Spindle speed, cutting velocity and tool path

The value of R-sq is 89.33% which shows the response flatness fits 89.33% in the model. 89.33% of the variability can be observed by the flatness.

The Model summary:

S	R-sq	R-sq(adj)	R-sq(pred)
0.0116872	89.33%	76.88%	38.56%

Table 4.5-1 4.5:1 Model summary for Flatness

The ANOVA analysis for surface roughness against process parameters are given below:

Source	DF	Adj SS	Adj MS	F-Value	P-Value
Model	14	0.013722	0.000980	7.18	0.001
Linear	4	0.005874	0.001468	10.75	0.001
overlapping percentage	1	0.005852	0.005852	42.84	0.000
spindle speed	1	0.000003	0.000003	0.02	0.885
cutting velocity	1	0.000012	0.000012	0.09	0.772
tool path	1	0.000007	0.000007	0.05	0.828
Square	4	0.007405	0.001851	13.55	0.000
overlapping percentage*overlapping percentage	1	0.001002	0.001002	7.34	0.019
spindle speed*spindle speed	1	0.000370	0.000370	2.71	0.126
cutting velocity*cutting velocity	1	0.000002	0.000002	0.02	0.897
tool path*tool path	1	0.006333	0.006333	46.36	0.000
2-Way Interaction	6	0.000444	0.000074	0.54	0.768
overlapping percentage*spindle speed	1	0.000000	0.000000	0.00	0.967
overlapping percentage*cutting velocity	1	0.000004	0.000004	0.03	0.867
overlapping percentage*tool path	1	0.000196	0.000196	1.43	0.254
spindle speed*cutting velocity	1	0.000225	0.000225	1.65	0.224
spindle speed*tool path	1	0.000002	0.000002	0.02	0.900
cutting velocity*tool path	1	0.000016	0.000016	0.12	0.738
Error	12	0.001639	0.000137		
Lack-of-Fit	10	0.001638	0.000164	491.53	0.002
Pure Error	2	0.000001	0.000000		
Total	26	0.015361			

Table 4.5-2 ANOVA between the flatness and process parameters

The ANOVA analysis between the flatness and the process parameters shows that the overall model is statistically significant with a P-value equal to 0.01. Whereas going through the individual parameters, the overlapping percentage is the most influencing factor for the flatness, while spindle speed has the least impact on the flatness of the workpiece. The two-way interaction of the process parameters has very little impact on the flatness. The maximum variation in flatness caused by the spindle speed*cutting velocity interaction is 77.6% out of a 95% confidence interval.

The empirical relation between flatness and process parameters is expressed as follows:

*Flatness = 0.030 - 0.00348 overlapping percentage - 0.000121 spindle speed + 0.00562 cutting velocity + 0.0016 tool path + 0.000034 overlapping percentage*overlapping percentage + 0.000000 spindle speed*spindle speed - 0.000007 cutting velocity*cutting velocity + 0.03446 tool path*tool path - 0.000000 overlapping percentage*spindle speed + 0.000005 overlapping percentage*cutting velocity + 0.000350 overlapping percentage*tool path - 0.000002 spindle speed*cutting velocity + 0.000002 spindle speed*tool path - 0.000200 cutting velocity*tool path*

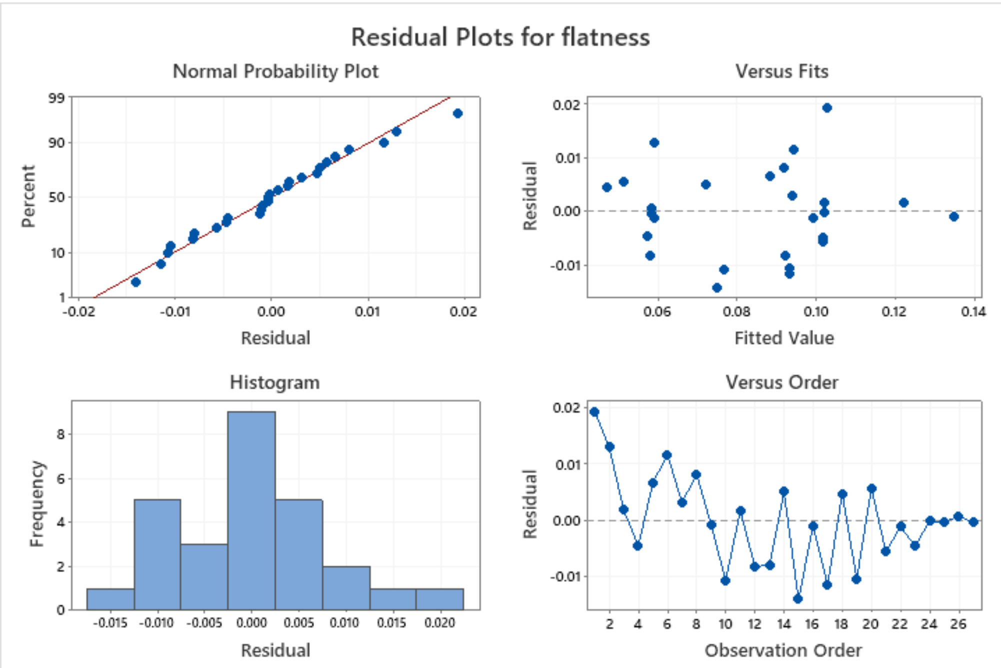

Figure 4.5:1 Residual Plots for Flatness

The residual plots shown in the figure 4.5:1, state that the residuals follow approximately a straight line with high number of residual very close to the line, indicates the normal distribution of the residual. The residual vs observation plot shows no obvious pattern therefor there is no violation of the uncorrelated variance in the model.

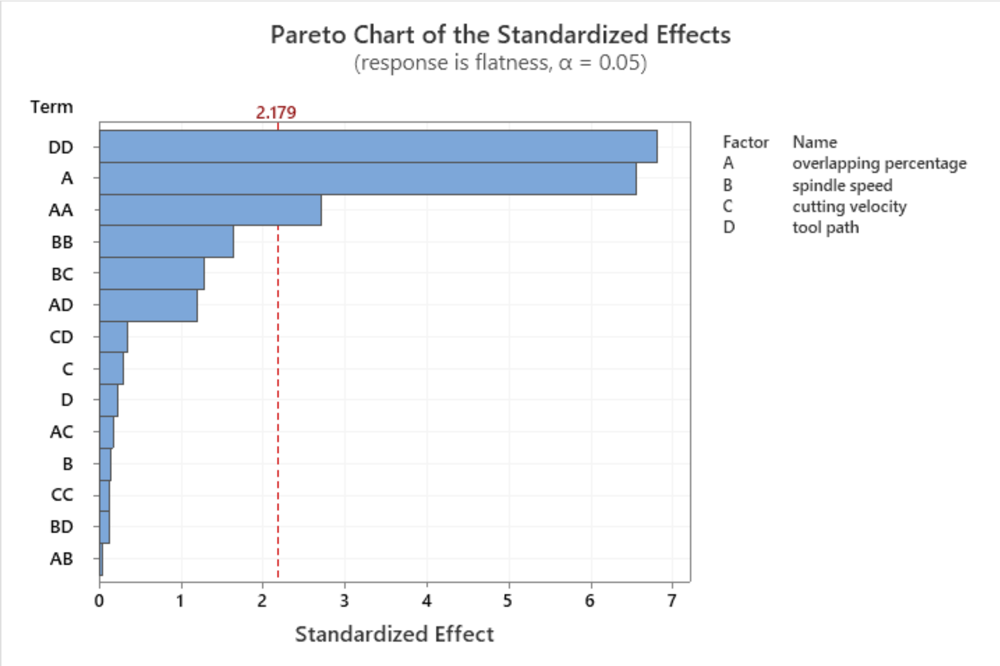

Figure 4.5:2 Pareto Chart for Flatness

According to the pareto chart for the response flatness, at alpha= 0.05, is highly influence by the square factor of tool path, followed by overlapping percentage and square factor of overlapping percentage.

4.6. Parallelism Vs Overlapping percentage, Spindle speed, cutting velocity and tool path

The Model summary:

The value of R-sq is 53.37% which shows the response parallelism fits 53.37% in the model. 53.37% of the variability can be observed by the parallelism.

S	R-sq	R-sq(adj)	R-sq(pred)
0.0610530	53.37%	0.00%	0.00%

Table 4.6-1 Model summary for Parallelism

The ANOVA analysis for parallelism against process parameters are given below:

Source	DF	Adj SS	Adj MS	F-Value	P-Value
Model	14	0.051189	0.003656	0.98	0.519
Linear	4	0.020163	0.005041	1.35	0.307
overlapping percentage	1	0.010740	0.010740	2.88	0.115
spindle speed	1	0.000867	0.000867	0.23	0.638
cutting velocity	1	0.000444	0.000444	0.12	0.736
tool path	1	0.008112	0.008112	2.18	0.166
Square	4	0.023356	0.005839	1.57	0.246
overlapping percentage*overlapping percentage	1	0.007138	0.007138	1.91	0.192
spindle speed*spindle speed	1	0.017608	0.017608	4.72	0.050
cutting velocity*cutting velocity	1	0.010247	0.010247	2.75	0.123
tool path*tool path	1	0.001002	0.001002	0.27	0.614
2-Way Interaction	6	0.007670	0.001278	0.34	0.901
overlapping percentage*spindle speed	1	0.002116	0.002116	0.57	0.466
overlapping percentage*cutting velocity	1	0.002756	0.002756	0.74	0.407
overlapping percentage*tool path	1	0.000625	0.000625	0.17	0.689
spindle speed*cutting velocity	1	0.000036	0.000036	0.01	0.923
spindle speed*tool path	1	0.000841	0.000841	0.23	0.643
cutting velocity*tool path	1	0.001296	0.001296	0.35	0.566
Error	12	0.044730	0.003727		
Lack-of-Fit	10	0.044725	0.004472	1916.78	0.001
Pure Error	2	0.000005	0.000002		
Total	26	0.095919			

Table 4.6-2 ANOVA between Parallelism and the process parameters

The ANOVA analysis between the parallelism and the process parameters shows that the overall model is not statistically significant with a P-value equal to 0.519, in other word, the model is 48.1% true instead of being 95% true.

but when going through the individual parameter's interaction with the parallelism, the overlapping percentage is 88.5% true instead of being 95% true, the spindle speed is 36.2% true instead of being 95% true, the cutting velocity is 26.4% true instead of being 95% true and the tool path is 83.4% true instead of being 95% true. This signify that the parameter, overlapping percentage and the tool path has higher interaction on the response parallelism in compared to the other two process parameters, i.e., cutting velocity and spindle speed. But going through the square factor, the ANOVA results shows that the square factor of spindle speed (spindle speed* spindle speed) has the p-value of 0.050 which is 95% true, which portray that the square factor of spindle speed has lot variance over parallelism when compared to other process parameter's square factors.

The empirical relation between parallelism and process parameters is expressed as follows:

*Parallelism = -4.83 + 0.0074 overlapping percentage + 0.00187 spindle speed + 0.0728 cutting velocity + 0.240 tool path - 0.000091 overlapping percentage*overlapping percentage - 0.000000 spindle speed*spindle speed - 0.000438 cutting velocity*cutting velocity - 0.0137 tool path*tool path + 0.000003 overlapping percentage*spindle speed - 0.000131 overlapping percentage*cutting velocity + 0.00062 overlapping percentage*tool path + 0.000001 spindle speed*cutting velocity - 0.000041 spindle speed*tool path - 0.00180 cutting velocity*tool path*

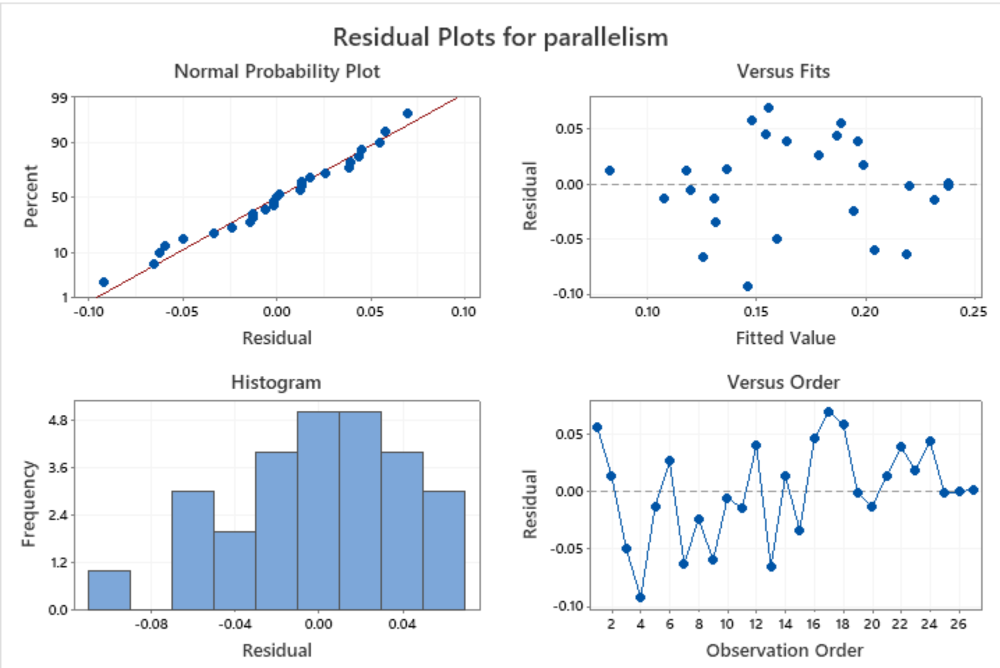

Figure 4.6:1 Residual Plots for Parallelism

The residual plots shown in the figure4.6:1, state that the residuals follow approximately a straight line with high number of residuals very close to the line, indicates the normal distribution of the residual. The residual vs observation plot shows no obvious pattern therefor there is no violation of the uncorrelated variance in the model.

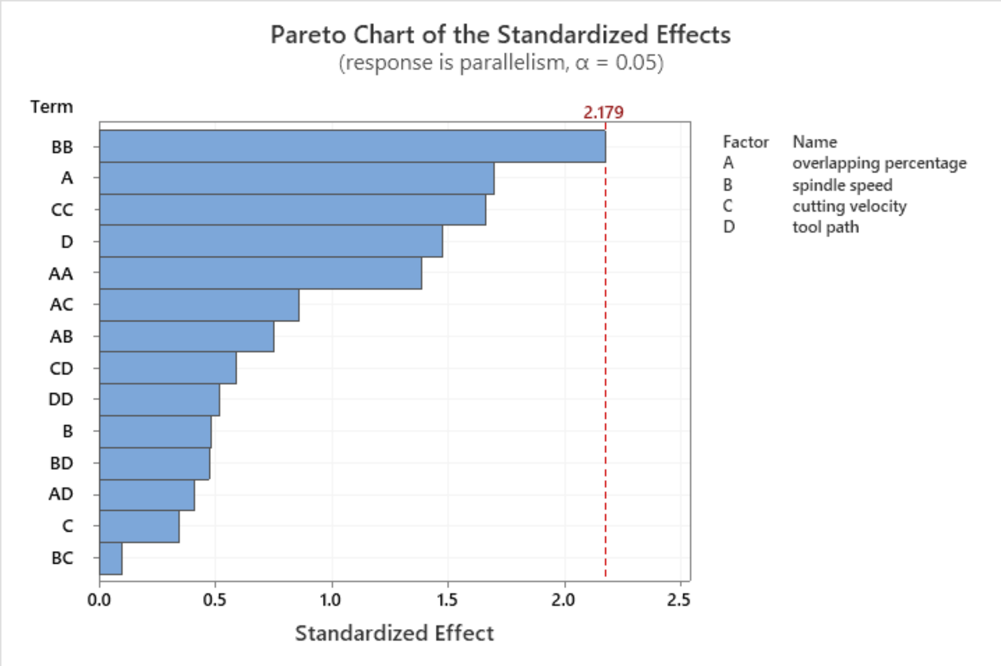

Figure 4.6:2 Pareto Chart for Parallelism

According to the pareto chart for the response parallelism, at alpha= 0.05, the square factor of spindle speed causes some influence in the parallelism, while the other process did not show any noticeable impact on the response parallelism.

4.7. MMR Vs Overlapping percentage, Spindle speed, cutting velocity and tool path

The Model summary:

The value of R-sq is 92.96% which shows the response MRR fits 92.96% in the model. 92.96% of the variability can be observed by the MRR.

S	R-sq	R-sq(adj)	R-sq(pred)
0.0115144	92.96%	84.75%	59.50%

Table 4.7-1 Model summary for Material Removal Rate

The ANOVA analysis for MRR against process parameters are given below:

Source	DF	Adj SS	Adj MS	F-Value	P-Value
Model	14	0.021008	0.001501	11.32	0.000
Linear	4	0.018523	0.004631	34.93	0.000
overlapping percentage	1	0.015827	0.015827	119.38	0.000
spindle speed	1	0.000000	0.000000	0.00	0.986
cutting velocity	1	0.002637	0.002637	19.89	0.001
tool path	1	0.000059	0.000059	0.44	0.517
Square	4	0.001966	0.000492	3.71	0.035
overlapping percentage*overlapping percentage	1	0.000146	0.000146	1.10	0.315
spindle speed*spindle speed	1	0.000000	0.000000	0.00	0.960
cutting velocity*cutting velocity	1	0.000172	0.000172	1.30	0.277
tool path*tool path	1	0.001169	0.001169	8.82	0.012
2-Way Interaction	6	0.000518	0.000086	0.65	0.689
overlapping percentage*spindle speed	1	0.000003	0.000003	0.02	0.882
overlapping percentage*cutting velocity	1	0.000111	0.000111	0.84	0.378
overlapping percentage*tool path	1	0.000055	0.000055	0.41	0.533
spindle speed*cutting velocity	1	0.000000	0.000000	0.00	0.969
spindle speed*tool path	1	0.000001	0.000001	0.01	0.922
cutting velocity*tool path	1	0.000348	0.000348	2.62	0.131
Error	12	0.001591	0.000133		
Lack-of-Fit	10	0.001588	0.000159	97.41	0.010
Pure Error	2	0.000003	0.000002		
Total	26	0.022599			

Table 4.7-2 ANOVA between MRR and process parameters

The ANOVA analysis between the MRR and the process parameters shows that the overall model is statistically significant with a P-value equal to 0.00. whereas going through the individual parameters, the overlapping percentage and the cutting velocity are the most influencing factor for the MRR while spindle speed is creating least impact on the MRR of the workpiece with a p-value of 0.986. The tool path is also not statistically significant for this model with a p-value of 0.517, which is 48.2% true instead of 100% but square factor of tool path has high impact on the MRR with a p-value of 0.012.

The empirical relation between MRR and process parameters is expressed as follows:

*MRR=0.418 + 0.00081 overlapping percentage - 0.000018 spindle speed - 0.00696 cutting velocity + 0.0859 tool path - 0.000013 overlapping percentage*overlapping percentage + 0.000000 spindle speed*spindle speed + 0.000057 cutting velocity*cutting velocity - 0.01480 tool path*tool path + 0.000000 overlapping percentage*spindle speed - 0.000026 overlapping percentage*cutting velocity - 0.000185 overlapping percentage*tool path + 0.000000 spindle speed*cutting velocity - 0.000002 spindle speed*tool path - 0.000932 cutting velocity*tool path*

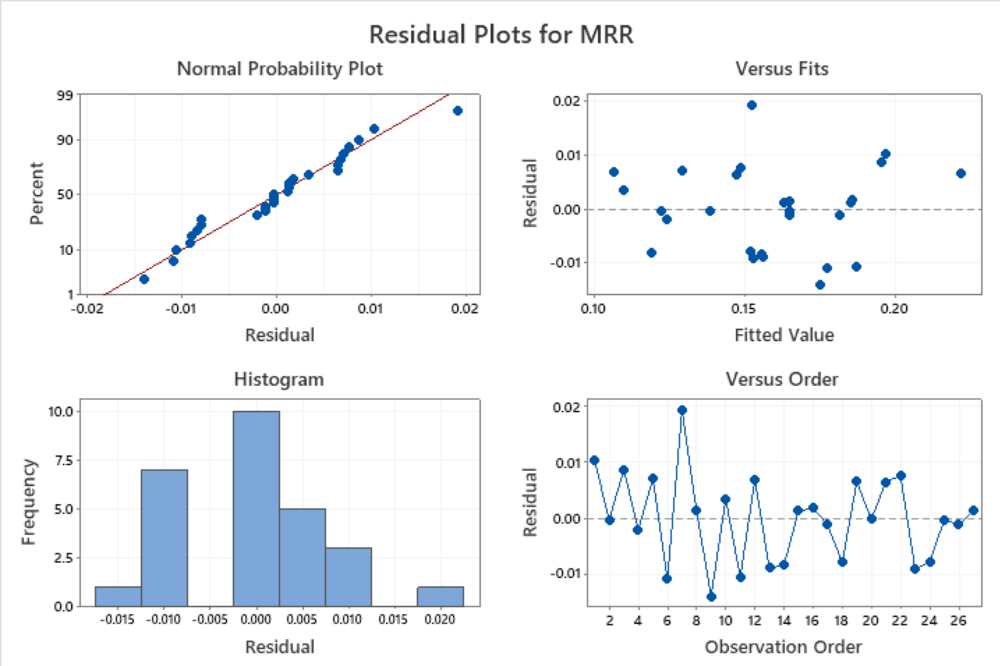

Figure 4.7:1 Residual Plots for Material Removal Rate

The residual plots shown in the figure 4.7:1, state that the residuals follow approximately a straight line with high number of residuals very close to the line, indicates the normal distribution of the residual. The residual vs observation plot shows no obvious pattern therefor there is no violation of the uncorrelated variance in the model.

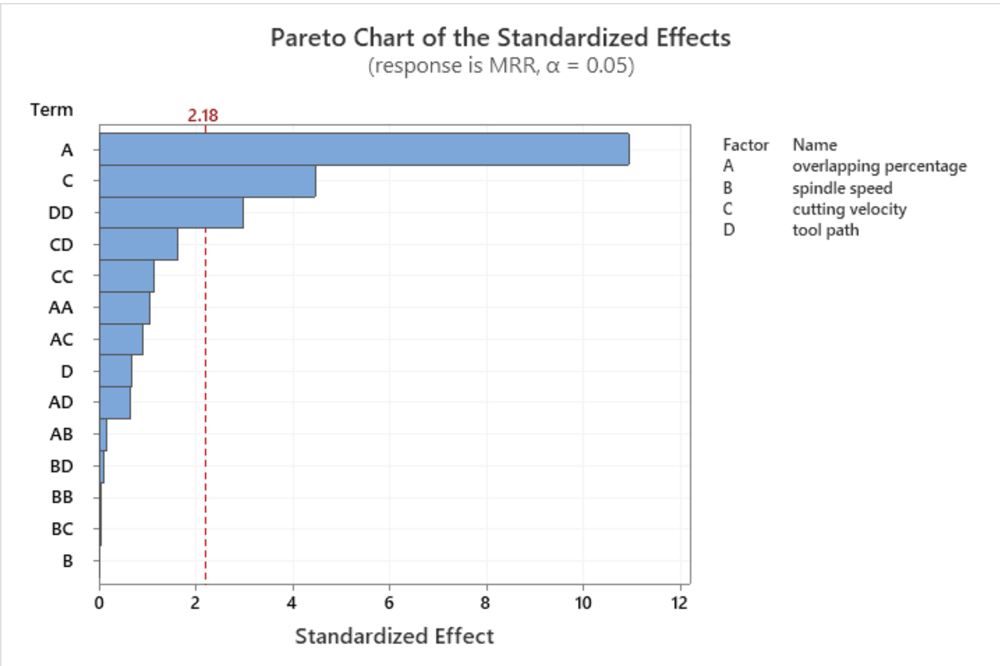

Figure 4.7:2 Pareto Chart for Material Removal Rate

According to the pareto chart for the response MRR, at alpha= 0.05, the maximum impact on MRR is cause by Overlapping percentage followed by cutting velocity. The chart also portray that the square factor of tool path has some influence on the MRR.

4.8. Machining Time Vs Overlapping percentage, Spindle speed, cutting velocity and tool path

The Model summary:

The value of R-sq is 99.27% which shows the response machining time fits 99.27% in the model. 99.27% of the variability can be observed by the machining time.

S	R-sq	R-sq(adj)	R-sq(pred)
46.5990	99.27%	98.42%	95.81%

Table 4.8-1 Model summary for Machining Time

The ANOVA analysis for Machining time against process parameters are given below:

Source	DF	Adj SS	Adj MS	F-Value	P-Value
Model	14	3552347	253739	116.85	0.000
Linear	4	3166569	791642	364.57	0.000
overlapping percentage	1	2597491	2597491	1196.19	0.000
spindle speed	1	3	3	0.00	0.971
cutting velocity	1	530881	530881	244.48	0.000
tool path	1	38194	38194	17.59	0.001
Square	4	357215	89304	41.13	0.000
overlapping percentage*overlapping percentage	1	123424	123424	56.84	0.000
spindle speed*spindle speed	1	6816	6816	3.14	0.102
cutting velocity*cutting velocity	1	120	120	0.06	0.818
tool path*tool path	1	187250	187250	86.23	0.000
2-Way Interaction	6	28563	4760	2.19	0.116
overlapping percentage*spindle speed	1	4	4	0.00	0.966
overlapping percentage*cutting velocity	1	12100	12100	5.57	0.036
overlapping percentage*tool path	1	7140	7140	3.29	0.095
spindle speed*cutting velocity	1	6	6	0.00	0.958
spindle speed*tool path	1	0	0	0.00	0.992
cutting velocity*tool path	1	9312	9312	4.29	0.061
Error	12	26058	2171		
Lack-of-Fit	10	26055	2605	1954.12	0.001
Pure Error	2	3	1		
Total	26	3578405			

Table 4.8-2 ANOVA between Machining time and process parameters

The ANOVA analysis between the machining time and the process parameters shows that the overall model is statistically significant with a P-value equal to 0.01. whereas going through the individual parameters, the spindle speed is the one of the very less influencing factors on the machining time with a p-value of 0.971 which is just 2.9% instead of being 95%%.

The empirical relation between Machining Time and process parameters is expressed as follows:

*Time = 798 + 22.8 overlapping percentage + 1.232 spindle speed - 6.0 cutting velocity + 378 tool path + 0.3803 overlapping percentage*overlapping percentage - 0.000292 spindle speed*spindle speed - 0.048 cutting velocity*cutting velocity + 187.4 tool path*tool path - 0.00014 overlapping percentage*spindle speed - 0.275 overlapping percentage*cutting velocity + 2.11 overlapping percentage*tool path + 0.00036 spindle speed*cutting velocity + 0.0007 spindle speed*tool path - 4.82 cutting velocity*tool path*

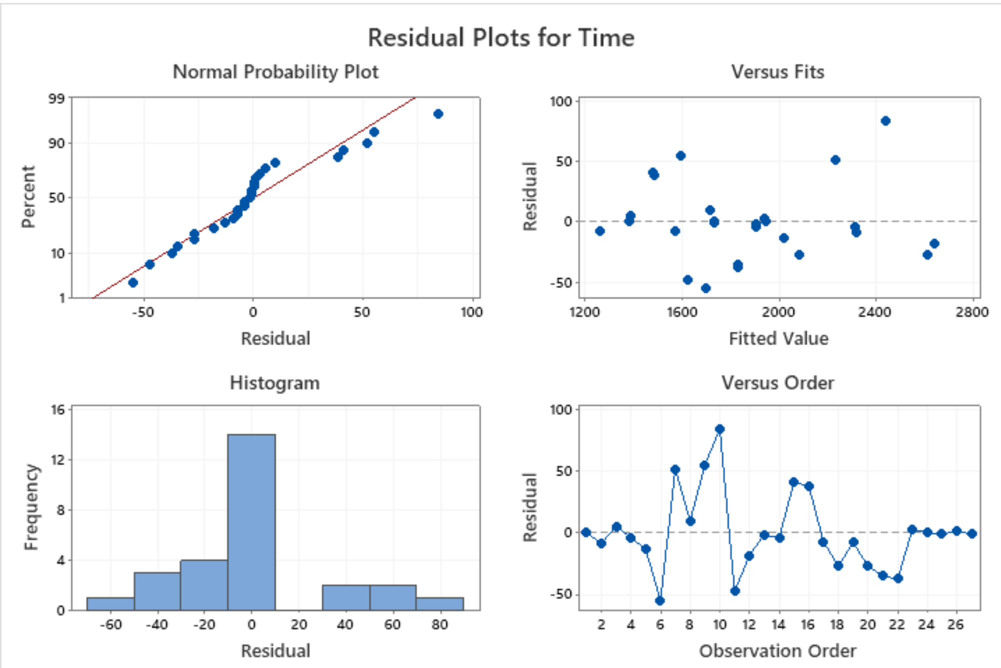

Figure 4.8:1 Residual Plots for Machining Time

The residual plots shown in the figure 4.8:1, state that the residuals follow approximately a straight line with high number of residuals very close to the line with some residual bit away from the normal line, indicates the normal distribution of the residual. The residual vs observation plot shows no obvious pattern therefor there is no violation of the uncorrelated variance in the model.

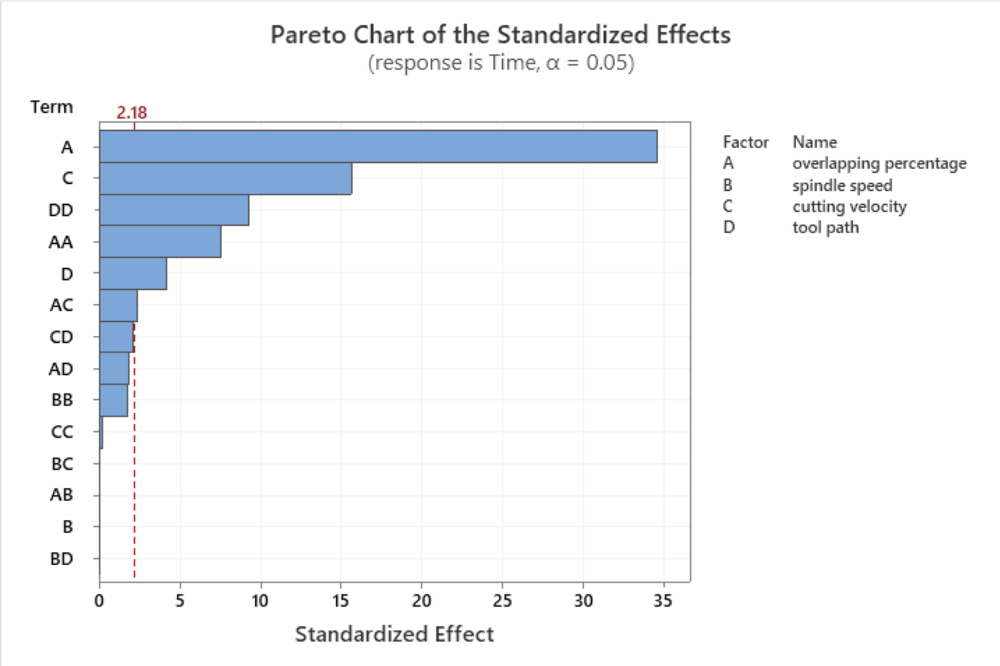

Figure 4.8:2 Pareto Chart for Machining Time

According to the pareto chart for the response Machining time, at alpha= 0.05, there is not any effect that are influencing the machining time because of the spindle speed whereas the maximum impact is due to overlapping percentage. Cutting velocity and tool path also shows good amount of impact on the machining time. There were some noticeable impact causes due to the square factor of tool path and the square factor of overlapping percentage. The two-way intersection of overlapping percentage- cutting velocity and cutting velocity and tool path are also causing some impact on the response MRR.

From the overall RSM analysis, it has been noticed that the models of the responses, flatness, MRR, and machining time are statistically significant, whereas the models for the responses, surface roughness, and parallelism are not statistically significant. For this, more experiments needed to be performed in order to conclude the behavior. Because it is a fact that with the variation of process parameters, the surface roughness will be influenced, but as per the model, there is a good amount of variation on the response but not as much to make the model statistically significant.

4.9. Optimization in Response Surface Methodology (RSM)

The optimization of this model is conducted on the same Minitab software, using RSM optimizer. The result from the optimizer is given below:

The predicted settings of the parameters for the optimum solution is portray in the table 4.9-1

Multiple Response Prediction

Variable	Setting
Overlapping percentage	26.5657
Spindle Speed	1800
Cutting Velocity	90
Tool path	-0.0505

Table 4.9-1 Predicted parameters settings

The optimum setting for overlapping percentage is 26.56%, spindle speed is 1800 which is the minimum spindle speed used in the experiment whereas the setting for the cutting velocity is 90 which is the maximum cutting speed used in the experiment whereas the tool path it is -0.0505.

Response	Value	Composite Desirability
Parallelism	0.1650	0.57137
Flatness	0.07923	0.66201
Machining time	1409.6	0.88609
Surface roughness	1.521	0.60154
MRR	0.19258	0.69664

Table 4.9-2 Optimization result obtains for predicted parameter setting

The optimization is carried out by keeping parallelism, flatness, machining time, surface roughness as minimum is better because minimum the value of these responses, better the surface quality will be, on the other hand for the response MRR, the setting was kept as maximum, because maximum the material removal rate will be, less machining and less power consumption will be utilized.

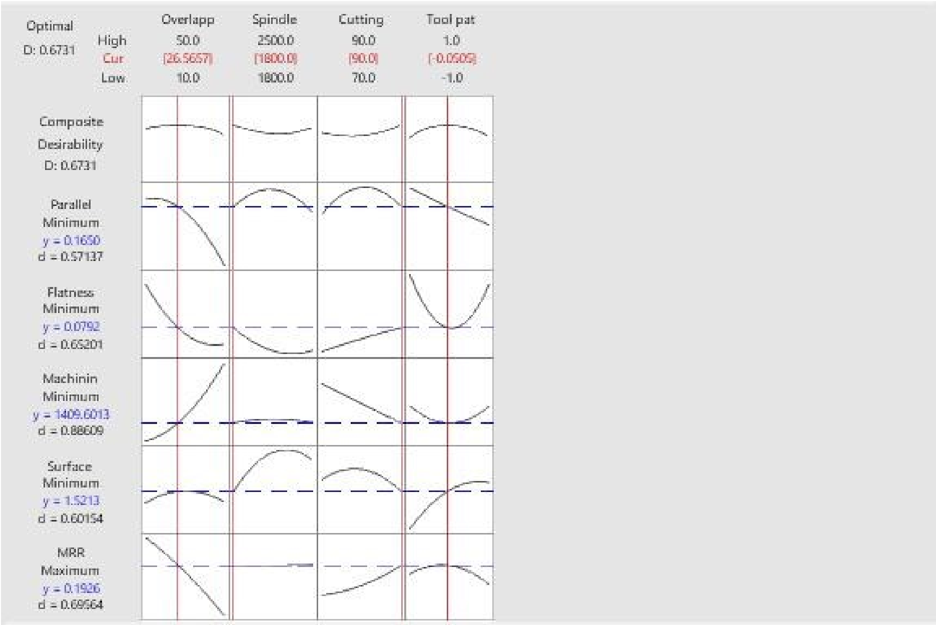

Figure 4.9:1 Optimization Plot

4.10. Validation test

To validate the results obtained from the RSM optimizer, a new experiment is performed with the exact parameters value obtained as predicted parameters setting given in table (). When going through the parameter setting, an issue with the tool path parameter arises because while forming the design of experiment, the three level of the tool path is -1,0 and 1 which is Counter, Zigzag and Spiral respectively, but the predicted value for the tool path is -0.0505 which is very closer to 0, so Zig-zag tool path technology is taken into account. To cross verify it a new experiment for validation with counter tool path was conducted but the result from this experiment causes higher deviation with the result obtained by considering zig-zag tool path. The results of validation test are given in the table4.10-1

Result			
Response	**RSM optimizer value**	**Validation test value**	**Deviation**
Surface Roughness	1.521	1.601	5.07%
Flatness	0.07923	0.077	2.5%
Parallelism	0.1650	0.146	12.12%
MRR	0.19258	0.19336	0.3%
Machining time	1409.6	1417	0.6%

Table 4.10-1 Validation test result

The flatness and Parallelism plot obtained from the CMM for the validation test are given in the figure 4.10:1 and figure 4.10:2, respectively.

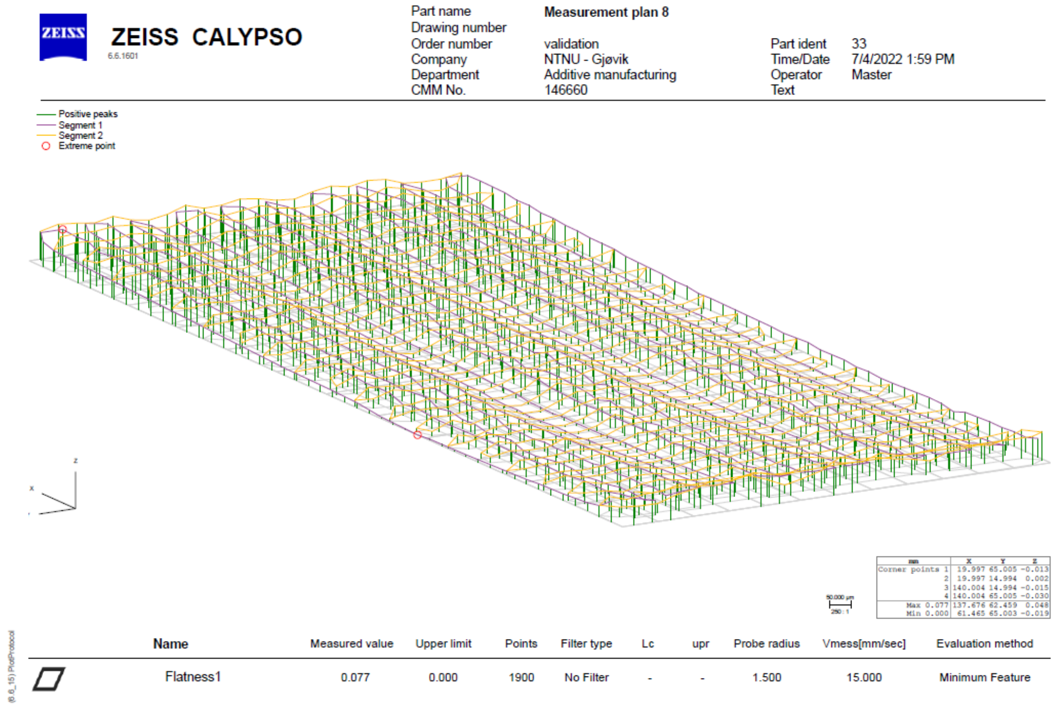

Figure 4.10:1 Flatness Plot for Validation test

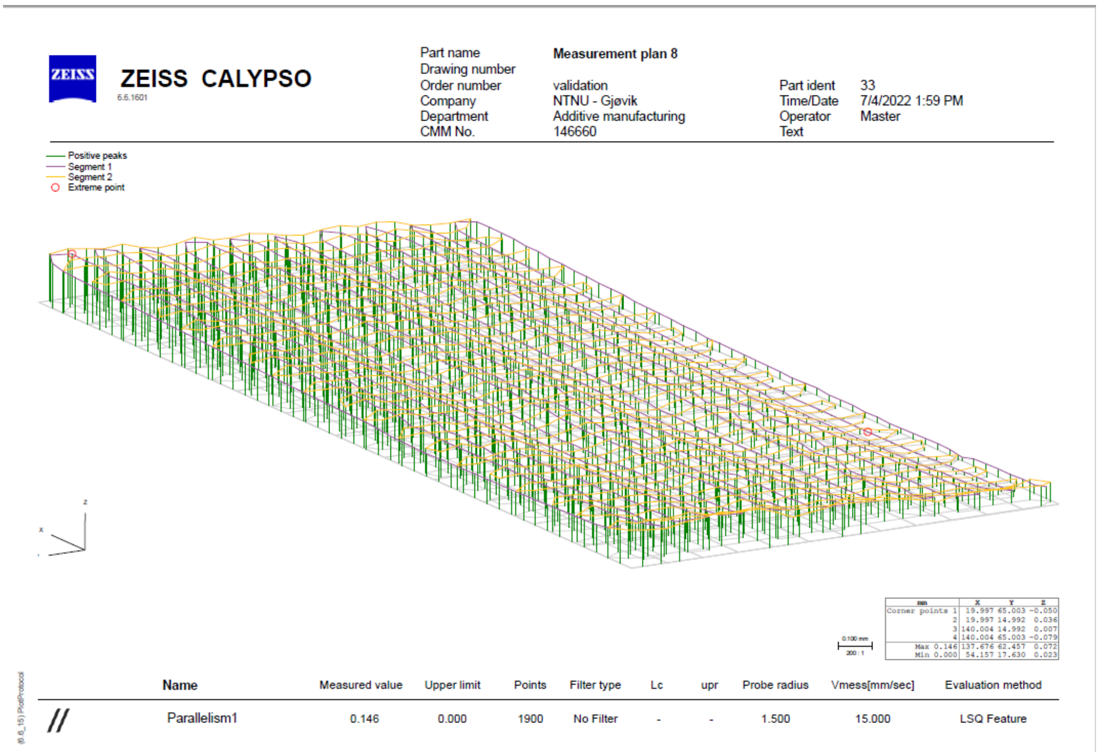

Figure 4.10:2 Parallelism plot for Validation test

Validation shows that roughness has 5.07% deviation from predicted values whereas Flatness, parallelism, MRR and Machining time have 2.5%, 12.12%, 0.3% and 0.6% deviations from predicted results. This also confirms that the result obtained using RSM are very close to the actual machining results.

5. Conclusion

CNC milling of Brass alloy has been performed successfully based on the Box-Behnken Design on the 160mm*80mm*15mm sample with the total of 27 experiments. Four different process parameter such as Spindle speed, cutting velocity, overlapping percentage of tool and tool path technology were chosen, whereas five different response parameter such as, surface roughness, flatness, parallelism, material removal rate by weight and machining time was kept for this study. Based on the result obtained from the experiment and the RSM the following conclusion can be made:

1. The analysis of variance result shows that the model for flatness, MRR and Machining time are statistically significant whereas the model for surface roughness and parallelism are not statistically significant at the confidence interval of 95% but in both case, there are good amount of variation caused by some of the individual process parameters.
2. The RSM optimizer shows that the optimum parameter combination, which are Overlapping Percentage = 26.57%, spindle speed = 1800 rpm, cutting velocity = 90 and tool path = zigzag and the predicted response values are surface roughness= 1.521-micron, flatness = 0.07923, parallelism = 0.1650, MRR = 0.19258 gm/sec and machining time = 1409.6 seconds.
3. The validation test results are surface roughness = 1.601-micron, flatness = 0.077, parallelism = 0.146, MRR = 0.19336 gm/sec and machining time = 1417 seconds. The result of flatness, parallelism and MRR are even better than the predicted value.
4. The deviation of validation test result against predicted result are surface roughness = 5.07%, flatness = 2.5%, parallelism = 12.12%, MRR = 0.3% and machining time = 0.6%, which also confirm that the result obtained from the RSM is very closer to the actual experimental results, making RSM as a proven method for the experiment carried out in this project.

6. Future Scope

- In this study, RSM model and ANOVA for the response parameters such as surface roughness and parallelism shows statistically not significant which can give an opportunity to extend this study further by conducting more experiment to find out their behaviors and the reason behind not being statistically significant.
- Using of different technology for getting surface response such as machine vision can also be one opportunity.
- Usually, every optimization has been done off-line, this opens scope for doing the optimization in-line in real time, for the application for manufacturing industries.

7. References

[1] R. Asadi, A. Yeganefar and S. A. Niknam, "Optimization and prediction of surface quality and cutting forces in the milling of aluminum alloys using ANFIS and interval type 2 neuro fuzzy network coupled with population-based meta-heuristic learning methods," *The International Journal of Advanced Manufacturing Technology,* vol. 105, p. 2271–2287, 2019.

[2] G. Ghosh, P. Mandal and S. C. Mondal, "Modeling and optimization of surface roughness in keyway milling using ANN, genetic algorithm, and particle swarm optimization," *The International Journal of Advanced Manufacturing Technology,* vol. 100, no. 1223–1242, 2019.

[3] P. K. Singh, P. Saini and D. Kumar, "Multi response optimization of CNC end milling of AISI H11 alloy steel for rough and finish machining using TGRA," *Materials Today: Proceedings,* vol. 26, no. 2, pp. 2564-2573, 2020.

[4] D. C. Montgomery, "Response Surface method and design," in *Design and Analysis of Experiments*, new jersey, John Wiley & Sons, Inc., 2019, pp. 408-430.

[5] K. Kadirgama, M. M. Noor and A. N. Abdalla, "Response Ant Colony Optimization of End Milling Surface Roughness," *Sensors,* vol. 10, no. 3, pp. 2054-2063, 2010.

[6] M. Farahnakian, M. Razfar, M. Moghri and M. Asadnia, "The selection of milling parameters by the PSO-based neural network modeling method," *International Journal of Advanced Manufacturing Technology,* vol. 57, pp. 49-60, 2011.

[7] J. Yan and L. Li, "Multi-objective optimization of milling parameters – the trade-offs between energy, production rate and cutting quality," *Journal of Cleaner Production,* vol. 52, no. 1, pp. 462-471, 2013.

[8] E. Kuram and B. Ozcelik, "Multi-objective optimization using Taguchi based grey relational analysis for micro-milling of Al 7075 material with ball nose end mill," *Measurement,* vol. 46, no. 6, pp. 1849-1864, 2013.

[9] A. R. Yildiz, "Cuckoo search algorithm for the selection of optimal machining parameters in milling operations," *The International Journal of Advanced Manufacturing Technology,* vol. 64, no. 1-4, pp. 55-61, 2013.

[10] L. M. Maiyar, R. Ramanujam, K. Venkatesan and J. Jerald, "Optimization of Machining Parameters for end Milling of Inconel 718 Super Alloy Using Taguchi based Grey Relational Analysis," *Procedia Engineering,* vol. 64, pp. 1276-1282, 2013.

[11] U. Yalcin, A. D. Karaoglan and I. Korkut, "Optimization of Cutting Parameters in Face Milling with Neural Networks and Taguchi based on Cutting Force, Surface Roughness and Temperatures," *International Journal of Production Research,* vol. 51, no. 11, pp. 3404-3414, 2013.

[12] T. P. Mahesh and R. Rajesh, "Optimal Selection of Process Parameters in CNC End Milling of Al 7075-T6 Aluminium Alloy Using a Taguchi-fuzzy Approach," *Procedia Materials Science,* vol. 5, pp. 2493-2502, 2014.

[13] I. Maher, M. E. H. Eltaib, A. A. D. Sarhan and R. M. El-Zahry, "Investigation of the effect of machining parameters on the surface quality of machined brass (60/40) in CNC end milling—ANFIS modeling," *The International Journal of Advanced Manufacturing Technology,* vol. 74, no. 1-4, pp. 531-537, 2014.

[14] M. K. Dikshit, A. B. Puri, A. Maity and A. J. Banerjee, "Analysis of Cutting Forces and Optimization of Cutting Parameters in High Speed Ball-end Milling Using Response Surface Methodology and Genetic Algorithm," *Procedia Materials Science,* vol. 5, pp. 1623-1632, 2014.

[15] T. Kıvak, "Optimization of surface roughness and flank wear using the Taguchi method in milling of Hadfield steel with PVD and CVD coated inserts," *Measurement,* vol. 50, pp. 19-28, 2014.

[16] J. S. Pang, M. N. M. Ansari, O. S. Zaroog, M. H. Ali and S. M. Sapuan, "Taguchi design optimization of machining parameters on the CNC end milling process of halloysite nanotube with aluminium reinforced epoxy matrix (HNT/Al/Ep) hybrid composite," *HBRC Journal,* vol. 10, no. 2, pp. 138-144, 2014.

[17] A. Nair, P. Govindan and H. Ganesan, "A Comparison between different Optimization Techniques for CNC End Milling Process," *Procedia Engineering,* vol. 97, pp. 36-46, 2014.

[18] M. S. Sukumar, P. V. Ramaiah and A. Nagarjuna, "Optimization and Prediction of Parameters in Face Milling of Al-6061 Using Taguchi and ANN Approach," *Procedia Engineering,* vol. 97, pp. 365-371, 2014.

[19] A. Alrashdan, O. Bataineh and M. Shbool, "Multi-criteria end milling parameters optimization of AISI D2 steel using genetic algorithm," *The International Journal of Advanced Manufacturing Technology,* vol. 73, no. 5-8, pp. 1201-1212, 2014.

[20] N. Masmiati and A. A. Sarhan, "Optimizing cutting parameters in inclined end milling for minimum surface residual stress – Taguchi approach," *Measurement,* vol. 60, pp. 267-275, 2015.

[21] Ş. Karabulut, "Optimization of surface roughness and cutting force during AA7039/Al2O3 metal matrix composites milling using neural networks and Taguchi method," *Measurement,* vol. 66, pp. 139-149, 2015.

[22] S. Zhenyu, L. Luning and L. Zhanqiang, "Influence of dynamic effects on surface roughness for face milling process," *The International Journal of Advanced Manufacturing Technology,* vol. 80, no. 9-12, p. 1823–1831, 2015.

[23] S. S. Bhogal, C. Sindhu, S. S. Dhami and B. S. Pabla, "Minimization of Surface Roughness and Tool Vibration in CNC Milling Operation," *Journal of Optimization,* p. 192030, 2015.

[24] P. Muñoz-Escalona and P. G. Maropoulos, "A geometrical model for surface roughness prediction when face milling Al 7075-T7351 with square insert tools," *Journal of Manufacturing Systems,* vol. 36, pp. 216-223, 2015.

[25] B. Das, S. Roy, R. N. Rai and S. C. Saha, "Application of grey fuzzy logic for the optimization of CNC milling parameters for Al–4.5%Cu–TiC MMCs with multi-performance characteristics," *Engineering Science and Technology, an International Journal,* vol. 19, no. 2, pp. 857-865, 2016.

[26] M. Sarıkaya, V. Yılmaz and H. Dilipak, "Modeling and multi-response optimization of milling characteristics based on Taguchi and gray relational analysis," *Proceedings of the Institution of Mechanical Engineers, Part B: Journal of Engineering Manufacture,* vol. 230, no. 6, pp. 1049-1065, 2016.

[27] N. Tamiloli, J. Venkatesan and B. V. Ramnath, "A grey-fuzzy modeling for evaluating surface roughness and material removal rate of coated end milling insert," *Measurement,* vol. 84, pp. 68-82, 2016.

[28] G. Xiang and Q. Zhang, "Multi-Object Optimization of Titanium Alloy Milling Process using Support Vector Machine and NSGA-II Algorithm," *International Journal of Simulation: Systems, Science and Technology,* vol. 17, no. 38, pp. 35.1-35.6., 2016.

[29] C. Li, Q. Xiao, Y. Tang and L. Li, "A method integrating Taguchi, RSM and MOPSO to CNC machining parameters optimization for energy saving," *Journal of Cleaner Production,* vol. 135, pp. 263-275, 2016.

[30] R. S. Altıntaş, M. Kahya and H. Ö. Ünver, "Modelling and optimization of energy consumption for feature based milling," *The International Journal of Advanced Manufacturing Technology,* vol. 86, no. 9-12, pp. 3345-3363, 2016.

[31] N. Zainal, A. M. Zain, N. Haizan, M. Radzi and M. R. Othman, "Glowworm swarm optimization (GSO) for optimization of machining parameters," *Journal of Intelligent Manufacturing,* vol. 27, pp. 797-804, 2016.

[32] Y. Xiong, J. Wu, C. Deng and Y. Wang, "Machining process parameters optimization for heavy-duty CNC machine tools in sustainable manufacturing," *The International Journal of Advanced Manufacturing Technology,* vol. 87, no. 5-8, p. 1237–1246, 2016.

[33] N. Masmiati, A. A. Sarhan, M. A. N. Hassan and M. Hamdi, "Optimization of cutting conditions for minimum residual stress, cutting force and surface roughness in end milling of S50C medium carbon steel," *Measurement,* vol. 86, pp. 253-265, 2016.

[34] A. Shokrani, V. Dhokia and S. T. Newman, "Comparative investigation on using cryogenic machining in CNC milling of Ti-6Al-4V titanium alloy," *Machining Science and Technology,* vol. 20, no. 3, pp. 475-494, 2016.

[35] M. Vardhan, G. Sankaraiah, M. Yohan and H. J. Rao, "Optimization of Parameters in CNC milling of P20 steel using Response Surface methodology and Taguchi Method," *Materials Today: Proceedings,* vol. 4, no. 8, pp. 9163-9169, 2017.

[36] R. L. Malghan, K. M. C. Rao, A. K. Shettigar, S. S. Rao and R. J. D’Souza, "Application of particle swarm optimization and response surface methodology for machining parameters optimization of aluminium matrix composites in milling operation," *Journal of the Brazilian Society of Mechanical Sciences and Engineering,* vol. 39, no. 9, p. 3541–3553, 2017.

[37] J. Zhou, J. Ren and C. Yao, "Multi-objective optimization of multi-axis ball-end milling Inconel 718 via grey relational analysis coupled with RBF neural network and PSO algorithm," *Measurement,* vol. 102, pp. 271-285, 2017.

[38] A. M. Khorasani and M. R. S. Yazdi, "Development of a dynamic surface roughness monitoring system based on artificial neural networks (ANN) in milling operation," *The International Journal of Advanced Manufacturing Technology,* vol. 93, no. 1-4, pp. 141-151, 2017.

[39] B. Rajeswari and K. S. Amirthagadeswaran, "Experimental investigation of machinability characteristics and multi-response optimization of end milling in aluminium composites using RSM based grey relational analysis," *Measurement,* vol. 105, pp. 78-86, 2017.

[40] A.-A. Selaimia, M. A. Yallese, H. Bensouilah, I. Meddour, R. Khattabi and T. Mabrouki, "Modeling and optimization in dry face milling of X2CrNi18-9 austenitic stainless steel using RMS and desirability approach," *Measurement,* vol. 107, pp. 53-67, 2017.

[41] C. Li, X. Chen, Y. Tang and L. Li, "Selection of optimum parameters in multi-pass face milling for maximum energy efficiency and minimum production cost," *Journal of Cleaner Production,* vol. 140, no. 3, pp. 1805-1818, 2017.

[42] J. Ribeiro, H. Lopes, L. Queijo and D. Figueiredo, "Optimization of Cutting Parameters to Minimize the Surface Roughness in the End Milling Process Using the Taguchi Method," *Periodica Polytechnica Mechanical Engineering,* vol. 61, no. 1, pp. 30-35, 2017.

[43] N. K. Sahu and A. B. Andhare, "Modelling and multiobjective optimization for productivity improvement in high speed milling of Ti–6Al–4V using RSM and GA," *Journal of the Brazilian Society of Mechanical Sciences and Engineering,* vol. 39, no. 12, p. 5069–5085, 2017.

[44] Ş. Karabulut and H. Karakoç, "Investigation of surface roughness in the milling of Al7075 and open-cell SiC foam composite and optimization of machining parameters," *Neural Computing and Applications,* vol. 28, no. 2, pp. 313-327, 2017.

[45] D. M. D. Costa, G. Belinato, T. G. Brito, A. P. Paiva, J. R. Ferreira and P. P. Balestrassi, "Weighted principal component analysis combined with Taguchi's signal-to-noise ratio to the multiobjective optimization of dry end milling process: a comparative study," *Journal of the Brazilian Society of Mechanical Sciences and Engineering,* vol. 39, no. 5, pp. 1663-1681, 2017.

[46] E. Kuram and B. Ozcelik, "Optimization of machining parameters during micro-milling of Ti6Al4V titanium alloy and Inconel 718 materials using Taguchi method," *Proceedings of the Institution of Mechanical Engineers, Part B: Journal of Engineering Manufacture,* vol. 231, no. 2, pp. 228-242, 2017.

[47] M. Mia, "Multi-response optimization of end milling parameters under through-tool cryogenic cooling condition," *Measurement,* vol. 111, pp. 134-145, 2017.

[48] R. B. D. Pereira, R. R. Leiteb, A. C. Alvim, A. P. d. Paiva, J. R. Ferreira and J. P. Davim, "Multi-objective robust optimization of the sustainable helical milling process of the aluminum alloy Al 7075 using the augmented-enhanced normalized normal constraint method," *Journal of Cleaner Production,* vol. 152, pp. 474-496, 2017.

[49] H. Zhang, Z. Deng, Y. Fua, L. Lv and C. Yan, "A process parameters optimization method of multi-pass dry milling for high efficiency, low energy and low carbon emissions," *Journal of Cleaner Production,* vol. 148, pp. 174-184, 2017.

[50] V. S. Kaushik, M. Subramanian and M. Sakthivel, "Optimization of Processes Parameters on Temperature Rise in CNC End Milling of Al 7068 using Hybrid Techniques," *Materials Today: Proceedings,* vol. 5, no. 2, pp. 7037-7046, 2018.

[51] R. Das, S. S. Mohanty, M. Panigrahi and S. Mohanty, "Predictive modelling and analysis of surface roughness in CNC milling of green alumina using response surface method and genetic algorithm," 2018.

[52] V. Gaikhe, J. Sahu and R. Pawade, "Optimization of Cutting Parameters for Cutting Force Minimization in Helical Ball End Milling of Inconel 718 by Using Genetic Algorithm," *Procedia CIRP,* vol. 77, pp. 477-480, 2018.

[53] Ş. Karabulut, U. Gökmen and H. Çinici, "Optimization of Machining Conditions for Surface Quality in Milling AA7039-Based Metal Matrix Composites," *Arabian Journal for Science and Engineering,* vol. 43, no. 3, pp. 1071-1082, 2018.

[54] S. Wojciechowski, R. W. Maruda, G. M. Krolczyk and P. Niesłony, "Application of signal to noise ratio and grey relational analysis to minimize forces and vibrations during precise ball end milling," *Precision Engineering,* vol. 51, pp. 582-596, 2018.

[55] D. B. Rao, K. V. Rao and A. G. Krishna, "A hybrid approach to multi response optimization of micro milling process parameters using Taguchi method based graph theory and matrix approach (GTMA) and utility concept," *Measurement,* vol. 120, pp. 43-51, 2018.

[56] R. Teimouri, S. Amini and A. B. Bami, "Evaluation of optimized surface properties and residual stress in ultrasonic assisted ball burnishing of AA6061-T6," *Measurement,* vol. 116, pp. 129-139, 2018.

[57] S. B. Sahare, S. P. Untawale, S. S. Chaudhari, R. L. Shrivastava and P. D. Kamble, "Optimization of End Milling Process for Al2024-T4 Aluminum by Combined Taguchi and Artificial Neural Network Process," in *Soft Computing: Theories and Applications. Advances in Intelligent Systems and Computing*, vol. 584, Pant, R. M., S. K., R. T. and B. A. S., Eds., Singapore, Springer, 2018, pp. 525-535.

[58] W. Mersni, M. Boujelbene, S. BenSalem and A.-S. Alghamdi, "Optimization of the surface roughness in ball end milling of titanium alloy Ti-6Al-4V using the Taguchi Method," *Procedia Manufacturing,* vol. 20, pp. 271-276, 2018.

[59] M. Mia, "Mathematical modeling and optimization of MQL assisted end milling characteristics based on RSM and Taguchi method," *Measurement,* vol. 121, pp. 249-260, 2018.

[60] J. U. Pillai, I. Sanghrajka, M. Shunmugavel, T. Muthuramalingam, M. Goldberg and G. Littlefair, "Optimisation of multiple response characteristics on end milling of aluminium alloy using Taguchi-Grey relational approach," *Measurement,* vol. 124, pp. 291-298, 2018.

[61] M. Sekulic, V. Pejic, M. Brezocnik, M. Gostimirovic and M. Hadzistevic, "Prediction of surface roughness in the ball-end milling process using response surface methodology, genetic algorithms, and grey wolf optimizer algorithm," *Advances in Production Engineering & Management,* vol. 13, no. 1, pp. 18-30, 2018.

[62] K. Aslantas, E. Ekici and A. Çiçek, "Optimization of process parameters for micro milling of Ti-6Al-4V alloy using Taguchi-based gray relational analysis," *Measurement,* vol. 128, pp. 419-427, 2018.

[63] C. Camposeco-Negrete and J. d. D. Calderón-Nájera, "Optimization of energy consumption and surface roughness in slot milling of AISI 6061 T6 using the response surface method," *The International Journal of Advanced Manufacturing Technology,* pp. 1-7, 2019.

[64] C. Li, L. Li, Y. Tang, Y. Zhu and L. Li, "A comprehensive approach to parameters optimization of energy-aware CNC milling," *Journal of Intelligent Manufacturing,* vol. 30, no. 1, pp. 123-138, 2019.

[65] A. M. Khan, M. Jamil, K. Salonitis, S. Sarfraz, W. Zhao, N. He, M. Mia and G. Zhao, "Multi-Objective Optimization of Energy Consumption and Surface Quality in Nanofluid SQCL Assisted Face Milling," *Energies,* vol. 12, no. 4, 2019.

[66] L. Peña-Parás, D. Maldonado-Cortés, M. Rodríguez-Villalobos, A. G.Romero-Cantú, O. E. Montemayor, M. Herrera, G. Trousselle, J. González and W. Hugler, "Optimization of milling parameters of 1018 steel and nanoparticle additive concentration in cutting fluids for enhancing multi-response characteristics," *Wear,* Vols. 426-427, no. A, pp. 877-886, 2019.

[67] R. A. Ali, M. Mia, A. M. Khan, W. Chen, M. K. Gupta and C. I. Pruncu, "Multi-Response Optimization of Face Milling Performance Considering Tool Path Strategies in Machining of Al-2024," *Materials,* vol. 12, no. 7, p. 1013, 2019.

[68] R. B. D. Pereira, L. A. Silva, C. H. Lauro, L. C. Brandão, J. R. Ferreira and J. P. Davim, "Multi-objective robust design of helical milling hole quality on AISI H13 hardened steel by normalized normal constraint coupled with robust parameter design," *Applied Soft Computing,* vol. 75, pp. 652-685, 2019.

[69] E. Suneesh, "Multi-response optimisation of micro-milling parameters through GRA, TOPSIS and Taguchi techniques to increase production rate while reducing energy consumption," *Measurement,* 2019.

[70] Z. Li and Y. Shi, "Multi-Objective Parameter Optimization for Disc Milling Process of Titanium Alloy Blisk Channels," *Symmetry,* vol. 11, no. 2, p. 173, 2019.

[71] M. Jebaraj, M. P. Kumar, N. Yuvaraj and G. M. Rahman, "Experimental study of the influence of the process parameters in the milling of Al6082-T6 alloy," *Materials and Manufacturing Processes,* 2019.

[72] S. A. A. Daniel, R. Pugazhenthi, R. Kumar and S. Vijayananth, "Multi objective prediction and optimization of control parameters in the milling of aluminium hybrid metal matrix composites using ANN and Taguchi -grey relational analysis," *Defence Technology,* 2019.

[73] T.-T. Nguyen, "Prediction and optimization of machining energy, surface roughness, and production rate in SKD61 milling," *Measurement,* vol. 136, pp. 525-544, 2019.

[74] R. Asadi, A. Yeganefar and . S. A. Niknam, "Optimization and prediction of surface quality and cutting forces in the milling of aluminum alloys using ANFIS and interval type 2 neuro fuzzy network coupled with population-based meta-heuristic learning methods," *The International Journal of Advanced Manufacturing Technology,* vol. 105, p. 2271–2287, 2019.

[75] A. T. Abbas, D. Y. Pimenov, . I. N. Erdakov, T. Mikolajczyk, . M. S. Soliman and M. . M. E. Rayes, "Optimization of cutting conditions using artificial neural networks and the Edgeworth-Pareto method for CNC face-milling operations on high-strength grade-H steel," *The International Journal of Advanced Manufacturing Technology,* vol. 105, p. 2151–2165, 2019.

[76] L. Imani, A. R. Henzaki, R. Hamzeloo and B. Davoodi, "Modeling and optimizing of cutting force and surface roughness in milling process of Inconel 738 using hybrid ANN and GA," *Journal of Engineering Manufacturing,* vol. 234, no. 5, pp. 920-932, 2019.

[77] P. K. Singh, P. Saini and D. Kumar, "Multi response optimization of CNC end milling of AISI H11 alloy steel for rough and finish machining using TGRA," *Materials Today: Proceedings,* vol. 26, no. 2, pp. 2564-2573, 2020.

[78] T. Ghosh, Y. Wang, K. Martinsen and K. Wang, "A surrogate-assisted optimization approach for multi-response end milling of aluminum alloy AA3105," *The International Journal of Advanced Manufacturing Technology,* vol. 111, pp. 2419-2439, 2020.

[79] B. Li, X. Tian and M. Zhang , "Modeling and multi-objective optimization of cutting parameters in the high-speed milling using RSM and improved TLBO algorithm," *The International Journal of Advanced Manufacturing Technology,* vol. 111, pp. 2323-2335, 2020.

[80] A. Muniappan, D. Maridurai, T. G. Sakthivel and C. Thiagarajan, "Modeling and analysis of CNC milling process parameters on surface integrity of aluminum hybrid composite," *Materials Today: Proceedings,* pp. 1-5, 2021.

[81] L.-H. Xu, C.-Z. Huang, . J.-H. Niu, J. Wang, H.-L. Liu and X.-D. Wang , "Prediction of cutting power and surface quality, and optimization of cutting parameters using new inference system in high-speed milling process," *Advances in Manufacturing,* vol. 9, pp. 388-402, 2021.

[82] I. P. Okokpujie, O. S. Ohunakin and C. A. Bolu, "Multi-objective optimization of machining factors on surface roughness, material removal rate and cutting force on end-milling using MWCNTs nano-lubricant," *Progress in Additive Manufacturing,* vol. 6, pp. 155-178, 2021.

[83] C. Feng, H. Guo, J. Zhang, Y. Huang and S. Huang , "A systematic method of optimization of machining parameters considering energy consumption, machining time, and surface roughness with experimental analysis," *The International Journal of Advanced Manufacturing Technology,* vol. 119, pp. 7383-7401, 2022.

[84] Ghoshouni industrial Co., "Material Datasheet CuZn39Pb2," GICO, Tehran, 2021.

[85] BDE Manufacturing Technologies, "Different Types of Dynamic Toolpaths to Optimize CNC Machining," BDE Manufacturing, Ave Beaverton, 2020.

[86] L. A. Sarabia and M. C. Ortiz, "1.12 - Response Surface Methodology," *Comprehensive Chemometrics,* pp. 345-390, 2009.

[87] R. Eyjolfsson, "Chapter-1: Introduction," in *Design and Manufacture of Pharmaceutical Tablets*, Academic Press, 2015, pp. 1-28.

[88] D. Panda, A. K. Satapathy and . S. K. Sarangi, "Multi-objective optimisation of thermodynamic performance parameters of a Gifford-McMahon refrigerator," *International Journal of Ambient Energy,* pp. 1-12, 2021.

[89] B. Ait-Amir, P. Pougnet and A. E. Hami, "6 - Meta-Model Development," *Embedded Mechatronic Systems 2,* pp. 157-187, 2020.

[90] Recurdyn V9R9, "AutoDesign / Basic Theory / Design of Experiments," Recurdyn V9R9, [Online]. Available: https://functionbay.com/documentation/onlinehelp/default.htm#!Documents/boxandbehnkendesignbbd.htm. [Accessed 1 July 2022].

[91] K. Palanikumar and J. P. Davim, "Electrical discharge machining: study on machining characteristics of WC/Co composites," *Machining and machine-tools,* pp. 135-168, 2013.

[92] N. A. A. Talib, F. Salam, N. A. Yusof, S. A. A. Ahmad and Y. Sulaiman, "Optimization of peak current of poly(3,4-ethylenedioxythiophene)/multi-walled carbon nanotube using response surface methodology/central composite design," *Royal Society of Chemistry,* vol. 7, pp. 11101-11110, 2017.

[93] zeiss, "Portable Surface Finish Measuring Instrument," *Handysurf E-35A/B,* p. 65.

[94] Zeiss, "Mobile Surface Measuring Instrument Featuring an elegant Design," zeiss- seeing beyond, [Online]. Available: https://www.zeiss.com/metrology/products/systems/form-and-surface/surface-measurement/handysurf.html. [Accessed 17 June 2022].

[95] T. Geiss, "flatness," GD&T Basic, 3 November 2014. [Online]. Available: https://www.gdandtbasics.com/flatness/. [Accessed 23 May 2020].

[96] Redlux, "Practical GD&T: Parallelism Measurement – Basic Concepts," red, United Kingdom, 2020.

[97] Q. Sun, X. Mu, J. Xu, W. Sun, L. Wang and Y. Yuan, "Substitutability analysis of a numerically simulated surface and an actual rough surface," *AIP Advances,* vol. 8, no. 8, p. 085022, 2018.

Appendix

Appendix A

G-code is a programming for CNC machine, which instruct machine where to move, which tool path to follow, at what feed rate the tool remove the materials. Below is the list of G-code of all the 27 experiments performed for this study

G-CODE

Appendix B

The 3D plot for the flatness and parallelism has been included below. The plot has been automatically generated from CMM. The plot shows the 3D representation of the measured Surface with all the measuring points.

CMM Plots

NTNU
Norwegian University of
Science and Technology